

The University of Maine

DigitalCommons@UMaine

---

Electronic Theses and Dissertations

Fogler Library

---


Spring 5-5-2023

## Synthesis of a Pharmaceutical Precursor from Bioderived Glucose

Justin O. P. Waters

University of Maine, [justin.o.waters@maine.edu](mailto:justin.o.waters@maine.edu)

Follow this and additional works at: <https://digitalcommons.library.umaine.edu/etd>

 Part of the [Biochemical and Biomolecular Engineering Commons](#), [Catalysis and Reaction Engineering Commons](#), and the [Organic Chemistry Commons](#)

---

### Recommended Citation

Waters, Justin O. P., "Synthesis of a Pharmaceutical Precursor from Bioderived Glucose" (2023).  
*Electronic Theses and Dissertations*. 3766.  
<https://digitalcommons.library.umaine.edu/etd/3766>

This Open-Access Thesis is brought to you for free and open access by DigitalCommons@UMaine. It has been accepted for inclusion in Electronic Theses and Dissertations by an authorized administrator of DigitalCommons@UMaine. For more information, please contact [um.library.technical.services@maine.edu](mailto:um.library.technical.services@maine.edu).

# **Synthesis of a Pharmaceutical Precursor from Bioderived Glucose**

By

Justin O. P. Waters

A.S. Engineering, NVCC 2020

A.S. Science, NVCC 2020

B.A. Foreign Language, UCONN 2009

A THESIS

Submitted in Partial Fulfilment of the  
Requirements for the Degree of  
Master of Science  
(In Chemical Engineering)

The Graduate School

The University of Maine

May 2023

## **Advisory Committee:**

Thomas J. Schwartz, Associate Professor of Chemical Engineering, Advisor

Sampath R. Gunukula, Assistant Research Professor – Forest Bioproducts Research Institute

M. Clayton Wheeler, Professor of Chemical Engineering

Copyright 2023 Justin O. P. Waters

All Rights Reserved

# **Synthesis of a Pharmaceutical Precursor from Bioderived Glucose**

By Justin O. P. Waters

Thesis Advisor: Dr. Thomas J. Schwartz

An Abstract of the Thesis Presented

In Partial Fulfillment of the Requirements for the

Degree of Master of Science

(In Chemical Engineering)

May 2023

Medication costs in the U.S. are high, and manufacturing and production comprise the largest share of those costs. As the world continues to shift to more sustainable methods of production, there are opportunities to reduce these costs through green synthesis. A large number of pharmaceuticals are derived from a precursor (S-3-hydroxy- $\gamma$ -butyrolactone 'HBL'). Drugs that treat cancer, antivirals, antibacterial drugs, and some cholesterol medications all can be derived from HBL.

Currently, HBL is almost exclusively derived from petroleum through an expensive and resource intensive process. Until recently, 'green' efforts to derive HBL from biomass have been plagued with many of the same inefficiencies as the petroleum.

The research outlined here takes a different approach. Through a series of two enzyme-catalyzed reactions we are able to synthesize a unique chemical intermediate, trione, from

biomass-derived glucose. This trione, through an additional series of base and acid-catalyzed reactions, can then be converted into our target chemical HBL.

Having proven the concept, continued research focused on the extraction of the target molecule from the acidic aqueous solution into an organic solvent. This organic solution is subsequently distilled to obtain pure HBL. Economic analysis of this process has been conducted and due to the low-cost feedstock, the enantiomeric selectivity, and the ease of extraction, costs for production at industrial scale are anticipated to be less than 50% of what is presently commercially available.

## **DEDICATION**

I would like to dedicate this thesis to my family and friends who have supported me along this journey.

To the friends I have been fortunate enough to find here at UMaine, thank you for your words of wisdom and counsel.

To my sisters Sasha and Krystina, without you having paved the way I wouldn't have known the journey was possible. I would have continued into adulthood always wishing I had pursued this dream which, thanks to you, is now a reality.

To my Dad, from a young age and even now into adulthood you have nurtured my love for science. You strove to always supply my inquisitive mind with greater and deeper insights and pushed me to ask tough questions and to seek those answers for myself. I am eternally grateful for your dedication, your patience, and for the sacrifices you made to provide me with limitless opportunity.

To my Mom, this is yours as much as it is mine. You never once let me give up and pushed me to keep climbing that mountain no matter how distant the peak seemed. At times when I slipped, you were there to catch me, and when I needed a hand to get back in the race, yours was always there. You are the north star of my success and I hope that in my endeavors I will continue to make you proud.

To my Bella, you are the best thing I've ever done with my life. I am so happy to start this new journey with you and to share with you all the exciting things I've learned as you grow and ask

questions about how the world works. I hope to be able to nurture your inquisitive mind in the same way that mine was so that you too can achieve your dreams whatever they may be.

## ACKNOWLEDGEMENTS

My work on this topic represents the most recent brick laid on a foundation of research that has stretched back many years across many institutions. However, consistent among the various researchers tasked with this undertaking, Dr. Thomas J. Schwartz, my advisor, has guided this project to its finish. I am grateful for his mentorship and for having welcomed me onto his research team despite my unconventional background. His support with learning how to navigate research in a laboratory environment, and his trust in my ability to accomplish the goals he set, helped me to grow and learn as a researcher and as a chemical engineer. I am grateful for his continued patience and understanding as I navigated school, research, and parenting. I am also grateful to Dr. Sampath R. Gunukula for his sage advice on future endeavors and for his patience in working with me to analyze the economics of the research outcomes. Finally, I would like to thank Dr. Clayton Wheeler for joining my advisory committee and for his feedback.

I am grateful for the research group alongside whom I have worked these past two years. Their help in learning the lab equipment, on best practices, and their feedback on my work were invaluable.

I am also grateful to the UMaine Catalysis Group. The time spent discussing existing research papers kept my mind sharp and the tools needed to complete my work were always at the forefront of my thinking. The tabletop discussions of shared research were crucial to surmounting hurdles we all faced in our various projects, and their feedback on my work ensured that no obstacle couldn't be reasoned through. In particular, I would like to thank Dr.



Brian Frederick for his patience in answering my many questions on various topics. I learn best through open discussion and his ability to narrate complex concepts in a digestible way made the learning process fun and accessible.

I couldn't have done the work I did without the foundation laid by my predecessors Elnaz Jamalzade and Hussein T. Abdulrazzaq; both from the UMaine graduate chemical engineering program. I must also thank my advisor Thomas J. Schwartz for his earlier work, James A. Dumesic from the University of Wisconsin-Madison, and Philip J. Kersten of the Forest Products Laboratory for their work on the enzyme catalyzed production of the trione intermediate and for their work in proving the background concept and obtaining funding.

I would like to thank the University of Maine Department of Chemical and Biomedical Engineering for welcoming me into their program, and the Forest Bioproducts Research Institute for providing the necessary laboratory space and equipment with which to conduct research.

## TABLE OF CONTENTS

DEDICATION.....	iii
ACKNOWLEDGEMENTS .....	v
LIST OF TABLES .....	ix
LIST OF FIGURES .....	x
LIST OF ABBREVIATIONS .....	xii

### CHAPTER

<b>1. INTRODUCTION .....</b>	<b>1</b>
Motivation .....	1
What is (S)-3-Hydroxy- $\gamma$ -Butyrolactone .....	2
Bioderived Glucose as a Starting Point .....	3
Petroleum Derived HBL.....	4
Alternative Chemical HBL Derivations .....	5
Biological Routes to HBL Production .....	6
Integrated Chemical-Biological Routes.....	6
<b>2. PROPOSED SYNTHESIS .....</b>	<b>8</b>
Methods.....	8
Enzyme Catalyzed Steps.....	8
Trione Monomer .....	10
Chemical Catalysis Steps .....	11
Base Catalysis.....	16
Acid Catalysis .....	22
Results & Discussion .....	24
<b>3. CHIRALITY OF SYNTHESIZED HBL .....</b>	<b>25</b>
Materials & Methods .....	25
Divergence of Chiral Peaks.....	28
Results & Discussion .....	30

<b>4. LIQUID-LIQUID EXTRACTION .....</b>	<b>31</b>
Materials & Methods .....	35
Results & Discussion .....	36
 <b>5. TECHNO-ECONOMIC ANALYSIS.....</b>	 <b>37</b>
Materials & Methods .....	37
Results & Discussion .....	39
 <b>6. CONCLUSION &amp; OUTLOOK .....</b>	 <b>41</b>
Recommendations for Future Work .....	41
 <b>7. REFERENCES.....</b>	 <b>43</b>
<b>8. APPENDIX .....</b>	<b>47</b>
<b>9. ABOUT THE AUTHOR .....</b>	<b>56</b>

## LIST OF TABLES

Table 1. Results of treatment of trione solution with bases of varying proton affinity as calculated .....	47
Table 2. Statistical analysis of $k_p$ value for ethyl acetate. ....	50
Table 3. Statistical analysis of $k_p$ value for THF .....	51
Table 4. Statistical analysis of $k_p$ value for propylene carbonate.....	51
Table 5. Total capital investment for the production of HBL.....	53
Table 6. Total process equipment costs for the production of HBL. ....	54
Table 7. Operating costs and discounted cash flow analysis assumptions.....	55

## LIST OF FIGURES

Figure 1. Enantiomers of HBL.....	2
Figure 2. D-glucose monomer (left) and cellulose polysaccharide (right).....	3
Figure 3. Close-up of plant leaf showing delineation of cell walls comprised of cellulose. (14) .....	3
Figure 4. Petroleum-derived commercial pathway for HBL synthesis.....	4
Figure 5. Proposed route from bioderived glucose to HBL via enzyme and chemical catalysis. (34) .....	8
Figure 6. POx enzyme catalyzed reaction of glucose to form glucosone. Peroxides are formed as a .....	9
Figure 7. Glucosone and peroxide side reactions and undesired byproducts.....	9
Figure 8. AUDH enzyme-catalyzed reaction of glucosone to form trione with depiction .....	10
Figure 9. AUDH enzyme-catalyzed dehydration of glucosone. (34) .....	11
Figure 10. Homogeneous base catalysts.....	12
Figure 11. Trione conversion (▲) and glycolate ester yield (●) over various sodium bicarbonate con ....	13
Figure 12. (a) Glycolate ester yield (▲) versus reaction time over tris base catalyst at 100% trione ) .....	14
Figure 13. (a): Glycolate ester yield (▲) versus reaction time over piperazine catalyst at 100% trion .....	15
Figure 14. Trione conversion (▲) and Glycolate ester yield (●) versus reaction time over bis tris .....	16
Figure 15. Potential reaction sequence by which trione is converted to the glycolate ester. (32).....	17
Figure 16. Glycolate ester TOF versus proton affinity (PA) of (▲) sodium bicarbonate, (▲)bis tris.....	18
Figure 17. Results from H-NMR reaction under conditions: 298K, 0.05M trione, 0.15M piperazine. ....	19
Figure 18. Structures of trione isomers and possible products of retro-aldol and hydrolysis reactions. ..	21
Figure 19. Kinetic model validation. Simulations (solid lines) based on the kinetic model (section a o. ...	21
Figure 20. Production yields of HBL from the acid catalyzed lactonization of DHB at 298K (orange), .....	23
Figure 21. Estimated product distribution of acid catalyzed lactonization of DHB to HBL at reaction. ....	23
Figure 22. Agilent 7820A Gas Chromatography System .....	26

Figure 23. Waters e2695 HPLC System .....	27
Figure 24. Inova 400 NMR System .....	27
Figure 25. Reaction network of enzyme and chemical catalyzed HBL synthesis with highlight.....	28
Figure 26. Gas chromatography with flame ionization detection (GC-FID) analysis of HBL enantiom. ....	29
Figure 27. Calculated partition coefficient for ethyl acetate extraction of HBL in aqueous solution. ....	32
Figure 28. Calculated partition coefficient for THF extraction of HBL in aqueous solution. ....	32
Figure 29. Calculated partition coefficient for propylene carbonate extraction of HBL in aqueous .....	33
Figure 30. Concentration of HBL synthesized in aqueous phase based on calculated $k_p$ values.....	34
Figure 31. Trione from batches 707-103 (left), and batches 707-112 (right). There are notable color. ....	35
Figure 32. Separatory funnels used in liquid-liquid HBL extraction. Organic phase (top).....	36
Figure 33. Process flow diagram for the production of HBL from glucose at 380kg/day production.....	38
Figure 34. Standard curve for H <sub>2</sub> O MilliporeSigma™ Supelco™ $\beta$ -Dex 255 capillary GC column con.....	48
Figure 35. Standard curve for THF MilliporeSigma™ Supelco™ $\beta$ -Dex 255 capillary GC column con.....	48
Figure 36. Standard curve for DMSO MilliporeSigma™ Supelco™ $\beta$ -Dex 255 capillary GC column . ....	49
Figure 37. Standard curve for EA MilliporeSigma™ Supelco™ $\beta$ -Dex 255 capillary GC column con.....	49
Figure 38. Standard curve for PC MilliporeSigma™ Supelco™ $\beta$ -Dex 255 capillary GC column con.....	50
Figure 39. GC-FID peaks for EA (top), THF (bottom), PC (right). EA appears to be more selective i .....	52

## LIST OF ABBREVIATIONS

AUDH	– Aldos-2-ulos Dehydratase
D2O	– Deuterium Oxide (Heavy Water)
DCF	– Discounted Cash Flow Method
DFT	– Density functional theory
DHB	– 3-4 Dihydroxybutyric Acid
DOE	– United States Department of Energy
EA	– Ethyl Acetate
FBRI	– Forest Bioproducts Research Institute
GA	– Glycolic acid
GC	– Gas Chromatography
GCFID	– Gas Chromatography with Flame Ionization Detection
GE	– Glycolate Ester
HBL	– (S)-3-Hydroxy- $\gamma$ -Butyrolactone
HCl	– Hydrochloric acid
HPLC	– High Performance Liquid Chromatography
Kp	– Partition Coefficient
NMR	– Nuclear Magnetic Resonance Spectroscopy (H – Hydrogen) ( $^{13}\text{C}$ – Carbon 13)
pA	– pico Amps
PA	– Proton affinity
PC	– Propylene Carbonate
POx	– Pyranose-2-oxidase
S	– Selectivity
TEA	– Techno-economic analysis
THF	– Tetrahydrofuran
X	– Conversion

The following chapters were adapted from: J.O.P. Waters, E. Jamalzade, H. Abdulrazzaq, J.A. Dumesic, P.J. Kersten, T.J. Schwartz, S.R. Gunukula. Can We Engineer Our Way To Cheaper Drugs? Synthesis of a Pharmaceutical Precursor from Bioderived Glucose. To be submitted in 2023. Manuscript drafted by Justin Waters who served as first author.

## Chapter 1

### INTRODUCTION

#### Motivation

Americans spend an estimated \$550 billion on pharmaceuticals each year (1). This staggering figure amounts to approximately \$1200 per year in per capita spending. However, this figure is skewed heavily towards those who do not require pharmaceuticals for their daily lives, with some paying upwards of \$10,000 monthly. These are totals that many already cannot afford. Insurance discounts, price concessions, rebates; these all serve to make an already unsustainable drug market more accessible (2). However, despite costs already outstripping the ability to pay, health industry analysts anticipate increased spending as national drug expenditures grow to a forecast \$621 billion by 2025 (1). While there is some debate as to whether rising drug costs in the U.S. match their production value, these forecasts warrant a deeper look into cost-cutting strategies.

According to a 2009 survey of the largest U.S. drug companies, materials and production were the greatest contributor to drug manufacturing costs, making this an ideal target for cost reduction efforts (3). One clear contender, (S)-3-hydroxy- $\gamma$ -butyrolactone (HBL), shows particular promise. HBL has been identified by the US Department of Energy (DOE) as an important platform chemical because of its broad use as a chemical intermediate (4) (5) (6). Moreover, this four-carbon compound is a crucial chiral building block in the synthesis of many pharmaceuticals, including cholesterol lowering drugs (*e.g.*, Lipitor and Crestor), antibiotics (*e.g.*, Linezolid and Ezetimibe), HIV inhibitors, and nutritional supplements, among others (7) (8)



(9) (10). Targeting this molecule for cheaper synthesis could potentially reduce the cost of downstream pharmaceuticals.

### What is (S)-3-Hydroxy- $\gamma$ -Butyrolactone

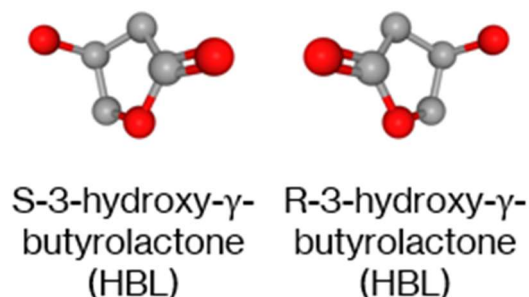


*Figure 1. Enantiomers of HBL*

To better understand why HBL is so critical it's important to characterize this molecule. HBL is a sweet-smelling small organic molecule prized for its amenability to further derivatization given that it contains both alcohols and carboxylic acids (in its linear form DHB). It is miscible with water and with some organic solvents though immiscible with light petroleum (11). This four-carbon chiral building block used in many facets of synthetic organic chemistry (12). To put into perspective the ubiquity and utility of this molecule, just one downstream drug, Lipitor, earned over \$2 billion in revenues for Pfizer in 2019. Prior to patent loss in 2011, this drug generated more than \$13 billion in revenues for Pfizer each year (13). And this is just one of many drugs which require HBL for synthesis.

It is derived from petrochemicals and biomass, particularly malic acids and carbohydrates.

However, petrochemical synthesis is expensive and difficult to purify. Despite these hurdles, it's flexibility means that there continue to be many market opportunities (12).

### Bioderived Glucose As A Starting Point

This research investigates the use of bioderived glucose as a cheap, renewable feedstock for HBL synthesis. The source of this glucose is cellulose, a long chain polysaccharide consisting of hundreds to thousands of d-glucose monomers (14).

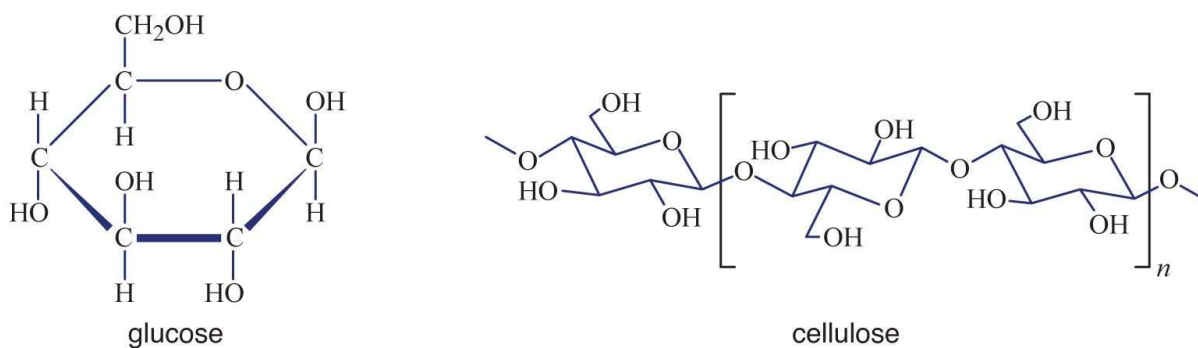


*Figure 2. D-glucose monomer (left) and cellulose polysaccharide (right).*

Cellulose makes up the cell walls of plants. It is renewable, in that it is created through photosynthetic growth processes of plants. Although it is not digestible, it is non-toxic to humans and is biodegradable (14).



*Figure 3. Close-up of plant leaf showing delineation of cell walls comprised of cellulose. (14)*

The cellulose is broken down into the necessary d-glucose monomers through a process called saccharification. This can be accomplished through chemical or enzyme catalyzed reactions which cleave the monomers from the polymer chain through hydrolysis (16). These sugars can then be used as renewable feedstock for downstream production processes.

### Petroleum Derived HBL

Presently, nearly all commercially available HBL is derived from petroleum, with wholesale costs reported to be *ca.* \$450/kg (4). This high cost is due largely to low production yields, costly purification processes, expensive starting materials, and catalyst deactivations with costly recovery. This is exacerbated by the use of hazardous materials (14) (15) (7) (12) (16).

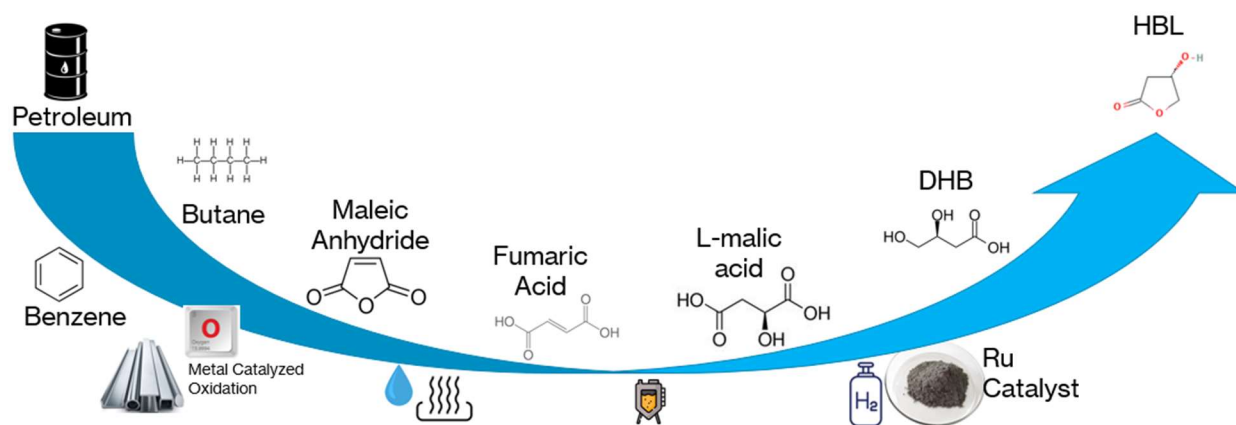


*Figure 4. Petroleum-derived commercial pathway for HBL synthesis*

Looking more closely at the process, commercial HBL is produced by catalytic reduction of L-malic acid with hydrogen using a supported Ru catalyst. The L-malic acid is obtained industrially by the enzyme-catalyzed hydration of fumaric acid (6) (17) (18) (19). This fumaric acid is itself a

derivative of maleic anhydride that is produced from butane or benzene (20) (21). The ruthenium catalyst used in this process, in addition to being expensive, is highly susceptible to deactivation, and the HBL produced is only chiral if the starting malic acid is enantiomerically pure (22) (23) (20). In general, the synthesis of HBL is difficult and limited by various factors consequential to the final selectivity (24).

### **Alternative Chemical HBL Derivations**

Two example routes to HBL were outlined in a 1998 patent application by Hollingsworth, which illuminate the difficulty in synthesis of this important chemical (24). In the first, the dimethyl ester of malic acid is reduced to (S)-1,2,4-butanetriol, and a dioxolane intermediate is created to protect the 1 and 3 hydroxyl groups. Following these steps, the 4-hydroxyl group is oxidized to an aldehyde and then to an acid. The acid is then deprotected and the dihydroxy compound is cyclized to HBL. The patent filing highlights that this process is intensive and has no commercial value as the dioxolane is contaminated with approximately 10% dioxane which is difficult to remove and results in the formation of 2-hydroxybutyrolactone contaminants. The second route outlined involves the direct reduction of malic acid to (S)-2-hydroxybutyric acid and the subsequent transformation to HBL. However, this reaction requires the use of a dimethyl sulfide complex of borane and a catalytic amount of sodium borohydride as the reducing system. Borane dimethyl sulfide requires specialized equipment to handle and an oxygen-free and moisture-free environment. It is highly toxic and expensive (18).

### **Biological Routes To HBL Production**

Conversely, biological catalysis presents opportunity for the production of biomass-derived molecules that can be upgraded into specialty chemicals. In a 2014 paper, Dhamankar, Tarasova, Martin and Prather outline a purely biosynthetic pathway to the production of HBL using glucose as the sole source of carbon. This process utilizes recombinant *Escherichia coli* and requires integration of endogenous glyoxylate shunt with the 3-4 dihydroxybutyric acid (DHB)/HBL pathway and co-overexpression of seven genes. While this method was proven successful, it faced some challenges. With respect to gene expression, repression of the glyoxylate shunt and optimal carbon distribution between the alternate pathway proved challenging. Optimizing yields also proved difficult. When given glucose test solutions of 15g/L, 10g/L, and 8g/L the cells were found to consistently use 5g/L of glucose for building biomass and for maintenance functions with remaining balances available for conversion. However, in the case of 8g/L, no HBL or DHB were produced, and in the case of 15g/L glucose solution, 5g/L was discovered to have gone unconsumed. After adjusting the experiments, the team ultimately achieved 0.3g/L HBL and 0.7g/L DHB, amounting to just 24% of the theoretical maximum (28).

### **Integrated Chemical-Biological Routes**

Recent studies highlight the promise of selective utilization of combined chemical and biological catalysis in upgrading biomass platforms (25) (26) (7) (27) (26) (28). However, these studies

reveal that several challenges need to be met to connect the two catalysis approaches: namely, the formation of biogenic impurities, and their negative impact on chemical catalyst performance (29) (27) (30) (31). We have previously used this approach to produce furyglycolic acid from glucose with 42% selectivity and 53% glucose conversion (27). Research suggests that a similar approach and technique to that outlined in the synthesis of furyglycolic acid can be used with minor changes in the reaction pathway to produce HBL from glucose (32) (33).

$$X_i = \frac{n_i(t=0) - n_i(t)}{n_i(t=0)} = 1 - \frac{n_i(t)}{n_i(t=0)}$$

*Equation 1. Conversion 'X' for a batch process is measured as the moles of reactant 'n' at 't=0' minus the moles of reactant at time 't' divided by the moles of reactant at time 't'.*

$$S_p = \frac{n_p(t)}{n_j(t)}$$

*Equation 2. Selectivity, 'S' for a batch process is defined as the ratio of the moles 'n' of desired product 'p', and the moles 'n' of undesired byproduct(s) 'j'.*

## Chapter 2

### PROPOSED SYNTHESIS

In this work, we show that enantiomerically pure S-HBL can be produced from glucose using a combination of whole-cell enzyme catalysis and homogeneous chemical catalysis, using a highly reactive species we refer to as 'trione' (see below) as an intermediate. An overview of the process is shown in the figure below.

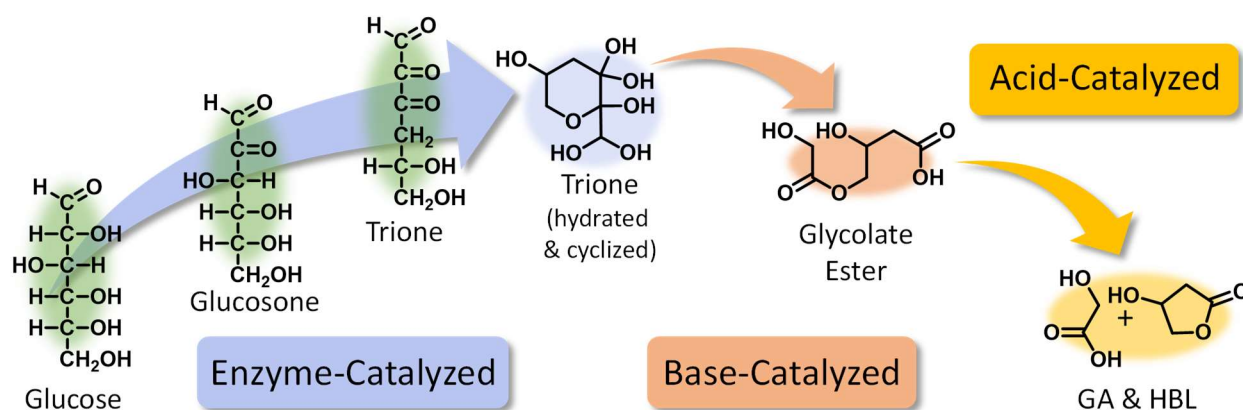


Figure 5. Proposed route from bioderived glucose to HBL via enzyme and chemical catalysis. (34)

### Methods

#### Enzyme-Catalyzed Steps

As depicted above, this process can be broken down into two sets of reactions, the first of which are referred to here as the 'biological stages'. These begin with the pyranose-2-oxidase (POx) enzyme catalyzed oxidation of glucose and conclude with the AUDH enzyme catalyzed conversion of glucosone to form trione (see above).

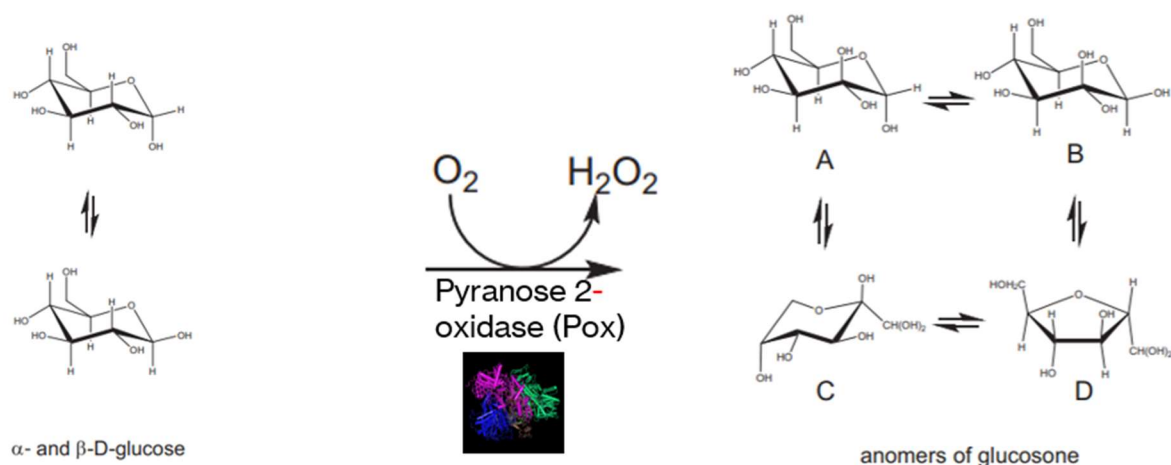


Figure 6. POx enzyme catalyzed reaction of glucose to form glucosone. Peroxides are formed as a byproduct of this reaction (37).

Biological stages begin with the enzyme catalyzed reaction of 0.555M glucose using pyranose-2-oxidase (POx), 11g wet cells per liter of solution, to form 0.555M glucosone with 100% conversion at 10hr at ambient temperatures. Catalase is added, 0.05g per liter of solution, to prevent peroxide formation and subsequent cell damage and yield losses.

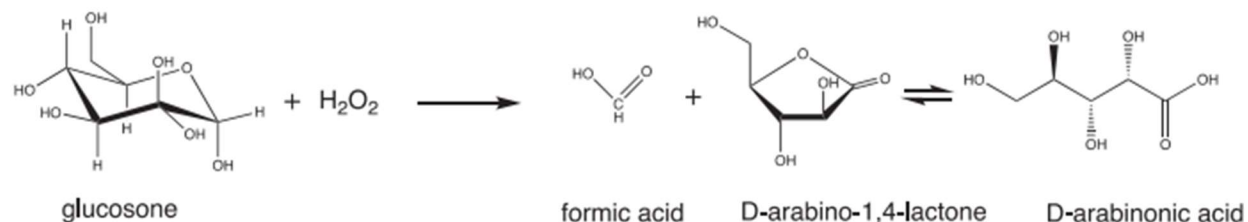
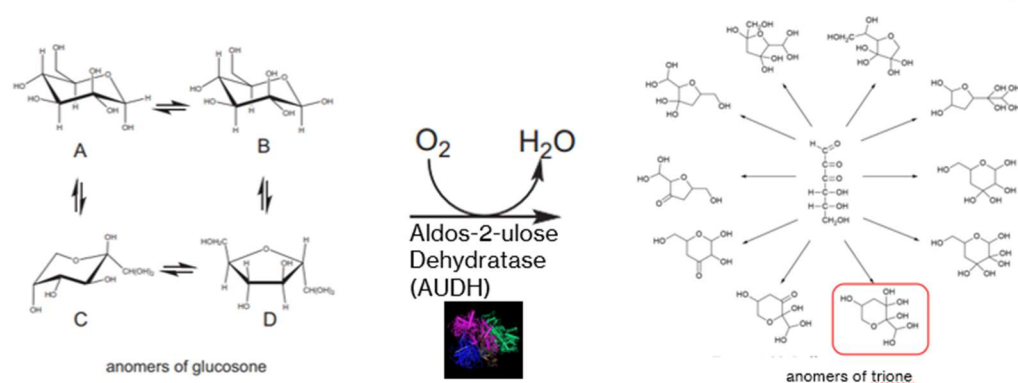


Figure 7. Glucosone and peroxide side reactions and undesired byproducts (37).

The resulting solution is centrifuged to remove live cells containing Pox enzymes for reuse in future reactions. To the supernatant, we add 41g/L genetically modified cells containing the enzyme aldose-2-ulose dehydratase (AUDH) to convert glucosone to our critical trione molecule.





*Figure 8. AUDH enzyme-catalyzed reaction of glucosone to form trione with depiction of glucosone and trione anomers. Circled is the hydrated and cyclized anomer of trione (37).*

This reaction similarly achieves 100% conversion at 18hr at ambient temperatures. The AUDH-containing cells are centrifuged and frozen for reuse, and the supernatant is subsequently upgraded directly using homogeneous base catalysts. Unlike with previously examined biological pathways, these molecules are synthesized free of growth medium components as washed cells are used and cell viability is not required for enzyme performance. Whole cells also eliminate the need for costly enzyme purification and immobilization (35).

### Trione Monomer

The resulting trione molecule is unique to this process, and crucial to the synthesis of the chiral HBL. The biocatalytic synthesis of trione occurs via the same pathway as the synthesis of cortalcerone (33). Where the two reactions differ is in a mutation in the 900-amino acid

sequence of AUDH which blocks enzymatic steps after the first dehydration. Without this mutation, glucosone would be converted to cortalcerone (see figure 9) (34).

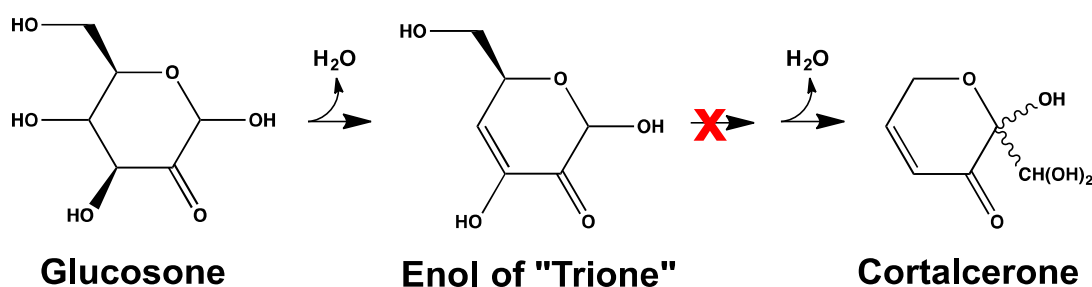


*Figure 9. AUDH enzyme-catalyzed dehydration of glucosone. (34)*

H- and  $^{13}\text{C}$ -NMR spectroscopy of the product solution suggests that trione exists as a distribution of 10 anomers, with the hydrated and cyclized anomer thought to be the most reactive species during subsequent chemical catalysis. We hypothesize that the distribution of these anomers is governed by equilibrium.

### Chemical Catalysis Steps

The trione solution is treated with a base catalyst to obtain an ester of glycolic acid and 3,4-dihydroxy-butryic acid (GE), which is subsequently hydrolyzed to yield 3,4-dihydroxybutyric acid (DHB) and glycolic acid (GA), with the DHB spontaneously lactonizing to produce HBL at low pH.

In this study we evaluated several base catalysts; sodium bicarbonate ( $\text{NaHCO}_3$ ) (Sigma Aldrich), tris base (Fisher Scientific), ultrapure bis-tris ( $\geq 98\%$  Dry Basis Fisher Scientific), piperazine (99% Extra Pure Acros Organics)

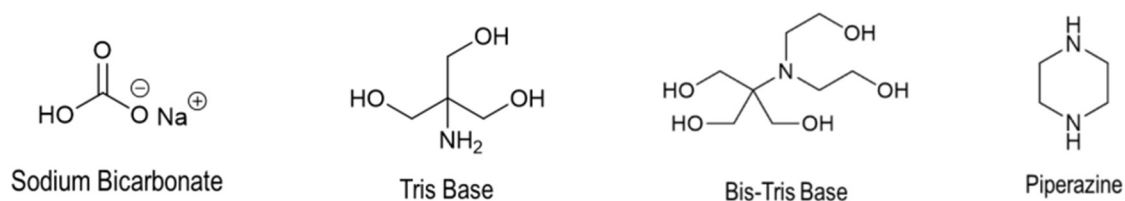


*Figure 10. Homogeneous base catalysts.*

Each catalyst was evaluated at 298 K, and under constant reaction conditions to evaluate catalyst activity and selectivity for glycolate esters (GE). Sodium bicarbonate achieved a maximum observed yield of GE of 91% at 0.3 M base concentration after 23 hours. The reaction was estimated to be first order with respect to the sodium bicarbonate catalyst at concentrations varying between 0.018 and 0.36 M.

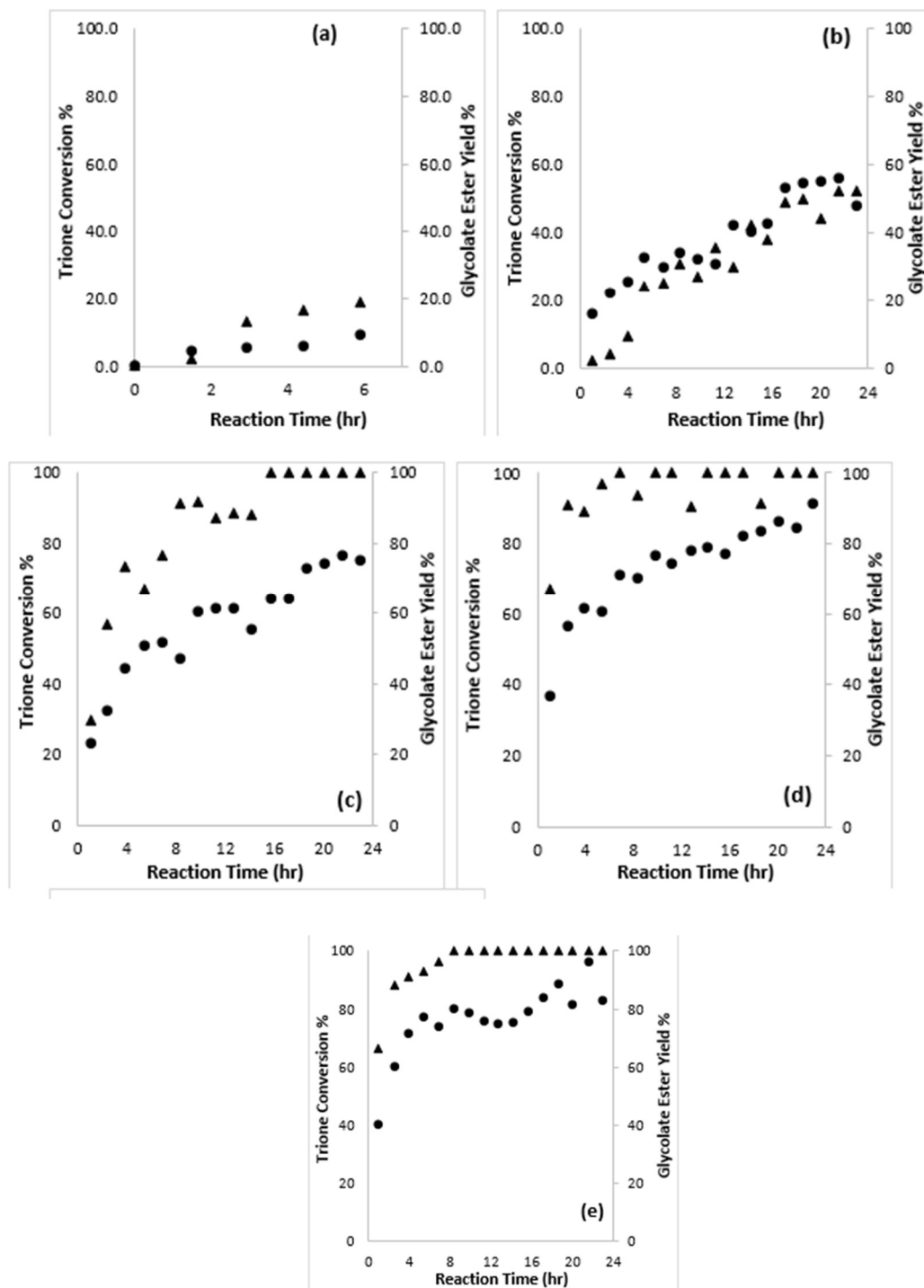


Figure 11. Trione conversion (▲) and glycolate ester yield (●) over various sodium bicarbonate concentrations (a) 0.03M, (b) 0.06M, (c) 0.18M, (d) 0.3M, and (e) 0.36M. Reaction conditions: 298 K reaction temperature, 0.156 mol/L trione, x mol/L NaHCO<sub>3</sub> (36)

Tris base ( $\text{C}_4\text{H}_{11}\text{NO}_3$ ) achieved complete conversion of trione in two hours at a base concentration of 0.3 M. However, GE formation peaked at 40%, dropping to less than 10% after nine hours corresponding to the GE undergoing hydrolysis to form the desired intermediate DHB and the byproduct, glycolic acid, at yields of 14% each.

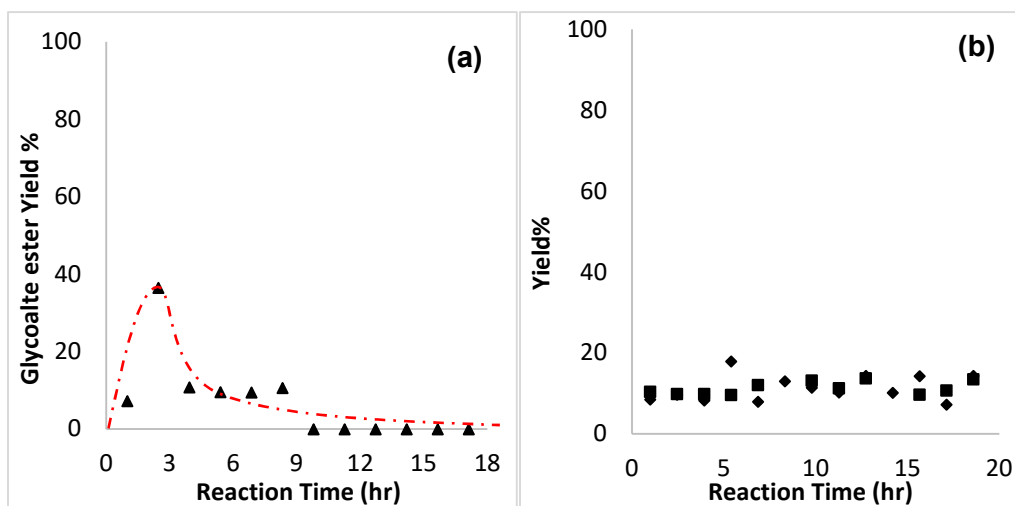


Figure 12. (a) Glycolate ester yield (▲) versus reaction time over tris base catalyst at 100% trione conversion. (b) Glycolic acid yield (■) and 3,4 DHB yield (◆) versus reaction time. Red dashed lines are used to guide the eye and do not correspond to any fit to this data. Reaction conditions: 0.156 mol/L trione, 0.3 mol/L base, and 298 K reaction temperature. (36)

Piperazine ( $\text{C}_4\text{H}_{10}\text{N}_2$ ) achieved complete conversion of trione at a base concentration of 0.3 M with GE yield peaking at approximately 23% after three hours. Within five hours, all GE was consumed through hydrolysis forming DHB and glycolic acid at 100% yield.

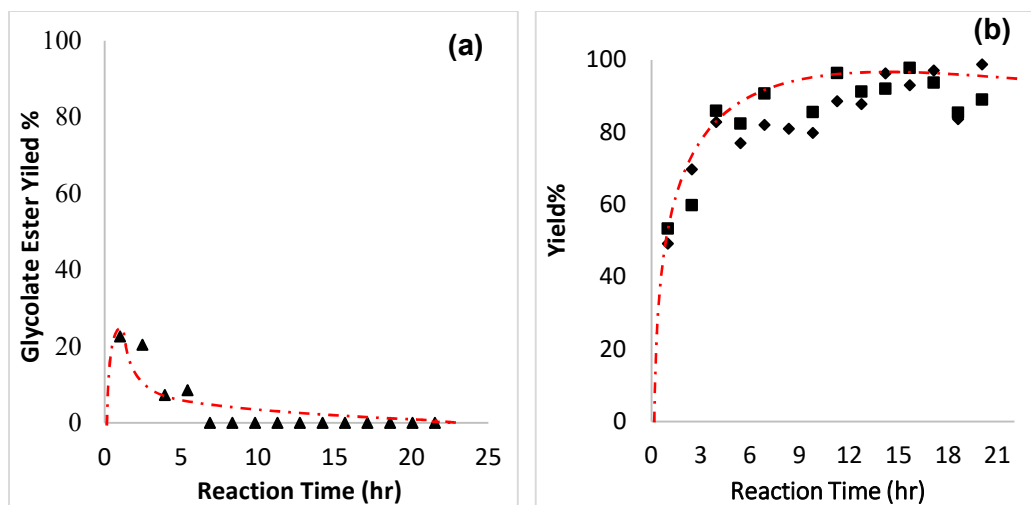


Figure 13. (a): Glycolate ester yield ( $\blacktriangle$ ) versus reaction time over piperazine catalyst at 100% trione conversion. (b): Glycolic acid yield ( $\blacksquare$ ) and 3,4 DHB yield ( $\blacklozenge$ ) versus reaction time. Red dashed lines are used to guide the eye and do not correspond to any fit to this data. Reaction conditions: 0.156 mol/L trione, 0.3 mol/L base and 298 K reaction temperature. (36)

Bis tris base ( $\text{C}_8\text{H}_{19}\text{NO}_5$ ) demonstrated complete conversion of trione at 11 hours with base concentration of 0.3 M and high yields (98%) for GE. There was no subsequent hydrolysis to form DHB and glycolic acid.

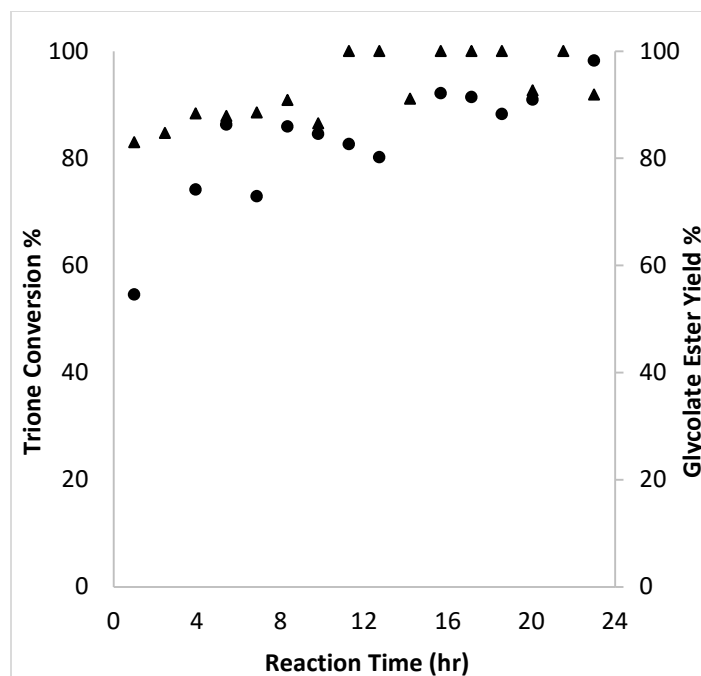


Figure 14. Trione conversion (▲) and Glycolate ester yield (●) versus reaction time over bis tris base catalyst. Reaction conditions: 0.156 mol/L trione, 0.3 M base, and 298 K reaction temperature. (36)

### Base Catalysis

The rate at which trione is converted to GE, and whether or not there is subsequent hydrolysis to form DHB, varies with the identity of the base catalyst. The retro-aldol reaction requires a carbonium ion transition state bound to the base catalyst, which suggests that the rate of C-C bond scission should scale with the strength of the base catalyst. This can be described by the proton affinity (PA), which was calculated using the ground state Density Functional Theory (DFT) method using Gaussian 16 software (37). The calculations were executed using Becke exchange functional and Lee-Yang-Parr correlation functional, supplemented with polarization diffuse function (6-311+G) as a basis set. The derived metric describes the basicity of a molecule and quantifies the thermodynamic gradient between a molecule and the anionic form of that

molecule upon proton extraction. The gradients are reaction and location dependent, meaning they are affected by the combination of reactants and the space occupied by the protons on a given acceptor. For analysis, the proton affinity was estimated as the difference between the total energies of the protonated and neutral form of the homogeneous bases. The resulting PA value was calculated based on the energy released during insertion of a proton to the Lewis acid center on the relaxed structure of the base molecules. (38) This quantification revealed that higher PA resulted in better yields of DHB (36).

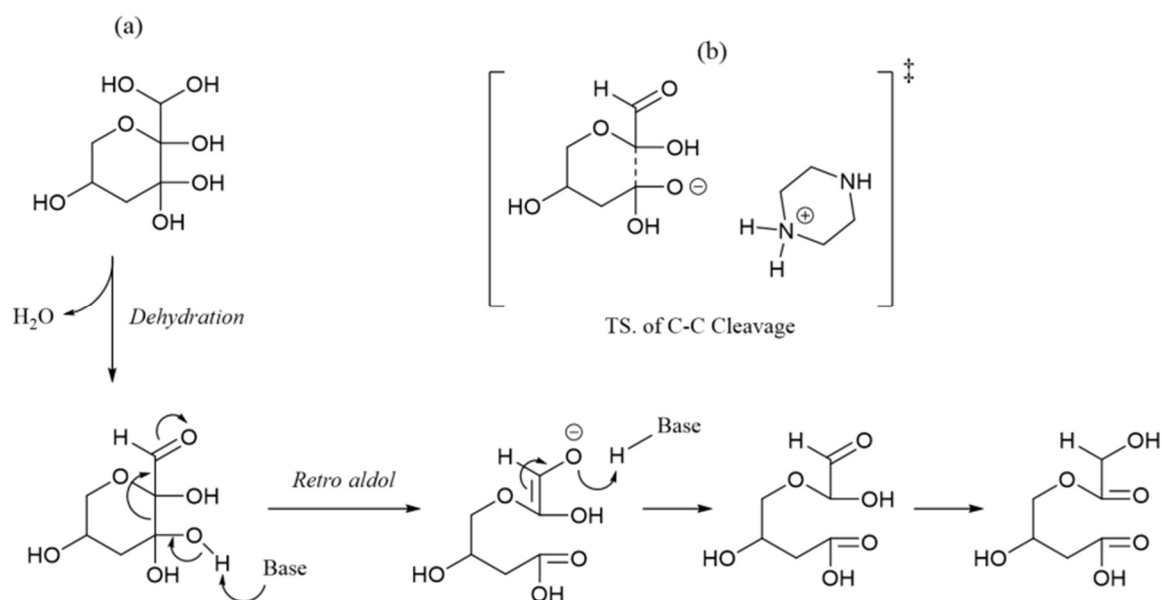


Figure 15. Potential reaction sequence by which trione is converted to the glycolate ester. (32)

Catalytic activity was determined by calculating the turnover frequency (TOF); the number of reactant molecules converted per minute per catalytic site (39). For this reaction it is defined as the rate of ester production normalized to the amount of homogeneous base catalyst present at low trione conversion and at low base concentration. The calculated TOF demonstrates high



activity for all four homogeneous bases, which is consistent with observation of complete conversion in all instances. This value scales linearly with the proton affinity of each base and suggests an optimum base strength for glycolate ester production (i.e. strong enough to achieve fast reactions but not so strong as to support subsequent hydrolysis). This too is consistent with comparative observations of maximum GE yield when plotted against proton affinity where the weakest (sodium bicarbonate) and the strongest (piperazine) bases showed maximum yields of 90% and 23% respectively. Given that piperazine facilitates ongoing hydrolysis its lower GE yield is preferable. The scaling shown suggests that the kinetically relevant transition state in ester formation is a carbonium ion as shown in the prior figure, stabilized by the Lewis base, which in turn is consistent with a retro-Aldol reaction being responsible for ester formation from trione.

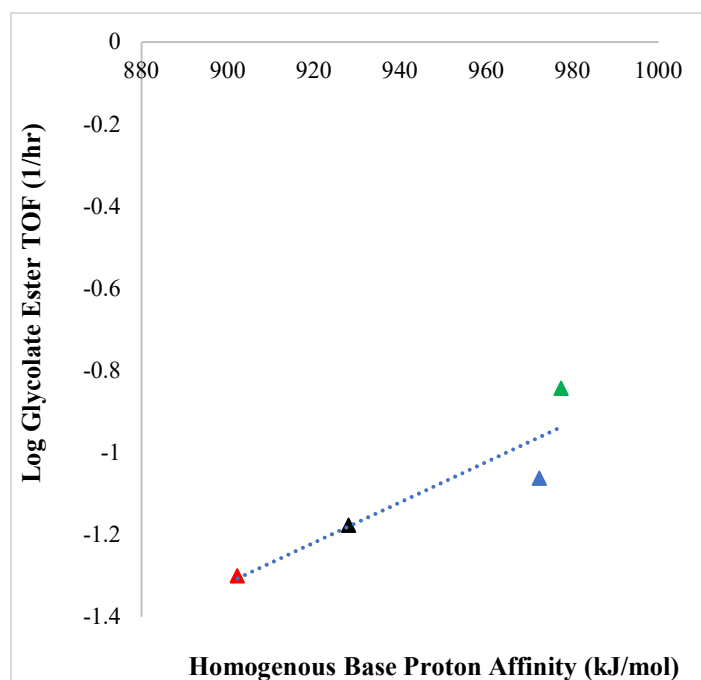


Figure 16. Glycolate ester TOF versus proton affinity (PA) of (▲) sodium bicarbonate, (▲)bis tris base, (▲) tris base, (▲) piperazine catalysts. Reaction conditions: 0.156 mol/L trione, 0.03 mol/L base, and 298 K reaction temperature (39).

Given the outcome of these experiments, piperazine was chosen for subsequent reactions. Use of this strong base ensured complete conversion and subsequent hydrolysis necessary for downstream reactions. Observation of the reaction using H-NMR analysis in previous work performed, shows the chemistry associated with the anomeric complexity of trione and the base catalyzed reaction and DHB formation (39).

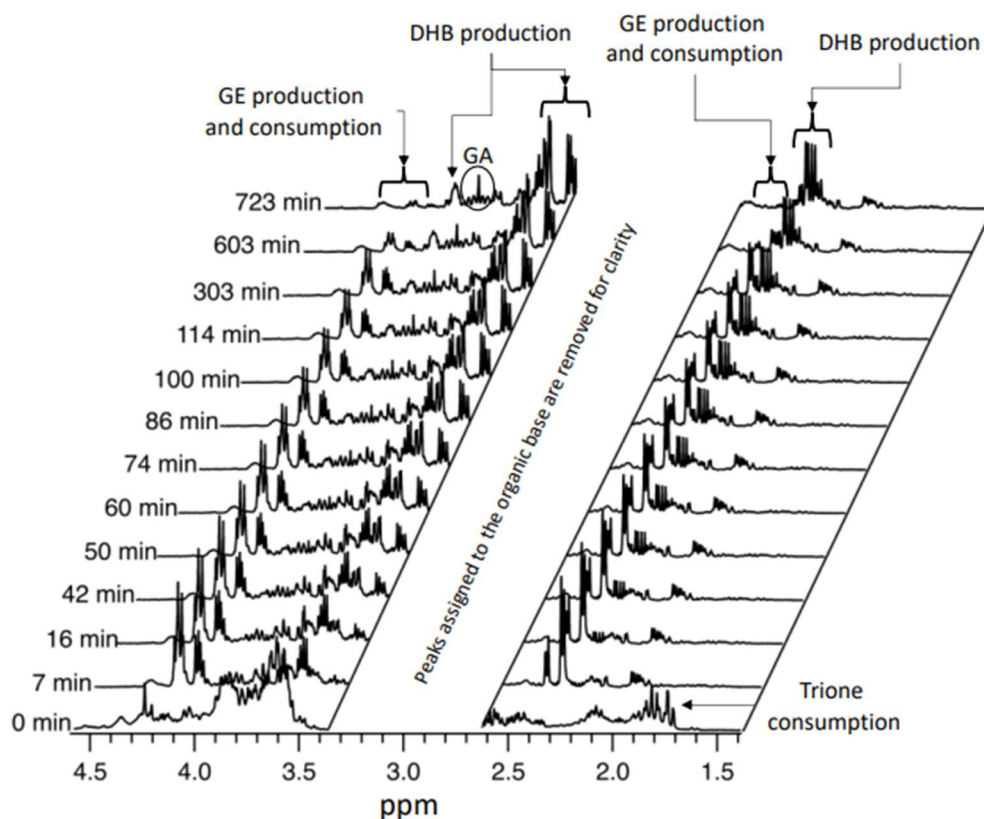


Figure 17. Results from H-NMR reaction under conditions: 298K, 0.05M trione, 0.15M piperazine (39).

Although the reaction network is complex, kinetic modeling of the proposed mechanism was developed that accurately tracks with experimental observations that could be made. The model was based on analysis of differential rate equations for each of the critical reactions that take place after homogeneous base catalyst is added to the trione solution. Solutions were based on the assumption that each step, trione > glycolate esters (GE) + polyols , and GE > DHB + GA, was first order and irreversible. Solutions obtained through numerical integration were fitted to the data to obtain rate constants for each step. Despite difficulties in quantifying these intermediate steps, what was observed experimentally through  $^{13}\text{C}$ -NMR and H-NMR matches closely with the proposed model. There are slight deviations from the model. These are attributed to inaccurate peak integrations during experimentation given that there is significant peak overlap. Efforts to resolve peaks failed to improve concentration measurements due to the persistence of polyol byproducts, and the presence of multiple trione anomers. Difficulty in obtaining a zero-point concentration of trione, again due to anomeric complexity, also contributed to error in closing carbon balances.

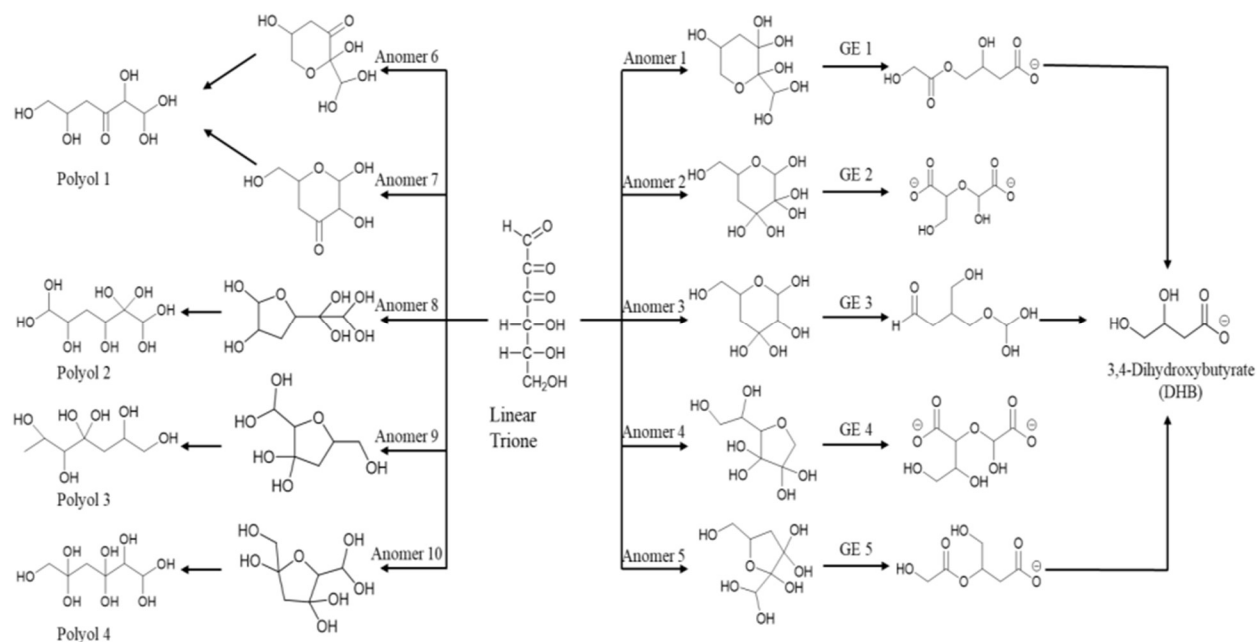


Figure 18. Structures of trione isomers and possible products of retro-aldol and hydrolysis reactions.

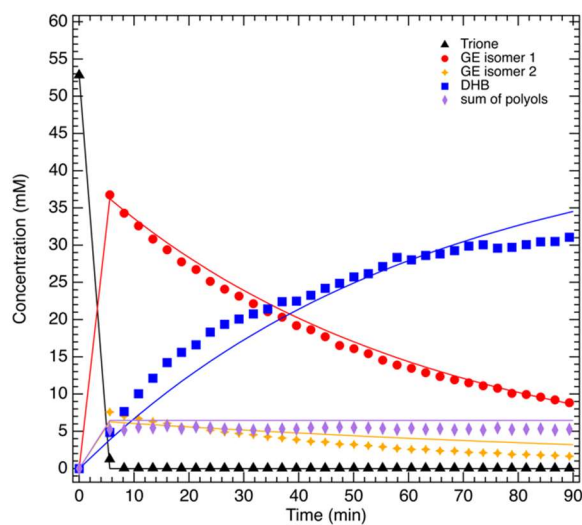


Figure 19. Kinetic model validation. Simulations (solid lines) based on the kinetic model (section a of this figure) at 298K (39).

## **Acid Catalysis**

It is well-documented in literature that lactonization reactions are acid-catalyzed and optimized at a pH of 0.7 (40) (41). With this knowledge, hydrochloric acid was added to the resulting DHB solution in amounts sufficient to drop the pH to the required levels. This was approximately 0.456 g of 12M HCl per 5ml of DHB solution. At the lower pH, lactonization occurs and DBH is converted to HBL. The reaction was studied at three different temperatures to optimize yields. A maximum yield of 88% was reached after 28 hours at 330K (36). Analysis of the resulting solution using heteronuclear single quantum coherence (HSQC) NMR, confirmed the presence of HBL and concentrations were estimated to be approximately 0.14M (36). Although there was some uncertainty around this figure due to potential error in peak integrations, later quantitative analysis using gas chromatography confirmed this concentration. We know, based on literature, that the lactonization reaction is equilibrium-limited, a fact that can be exploited during industrial production using a biphasic reactor. In such a scenario, HBL would be extracted in-situ from its aqueous reaction medium into the organic solvent allowing thermodynamic favorability to shift the equilibrium in favor of greater HBL production (42). This equilibrium is also impacted by temperature. At lower temperatures kinetic energies of reactant molecules decreases, lowering the overall reaction rate; however, if temperatures are too high the equilibrium shifts away from products and the lactones formed undergo hydrolysis to reform DHB as is evidenced by the following figure (43).

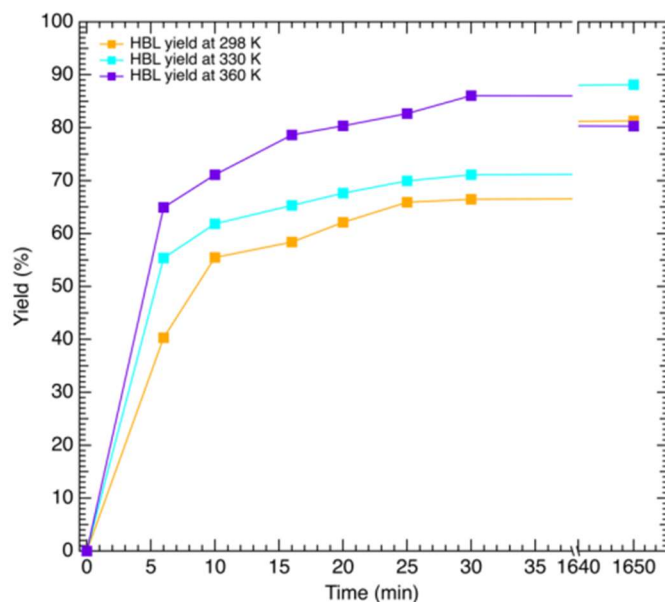


Figure 20. Production yields of HBL from the acid catalyzed lactonization of DHB at 298K (orange), 330K (blue), and 360K (purple) (39).

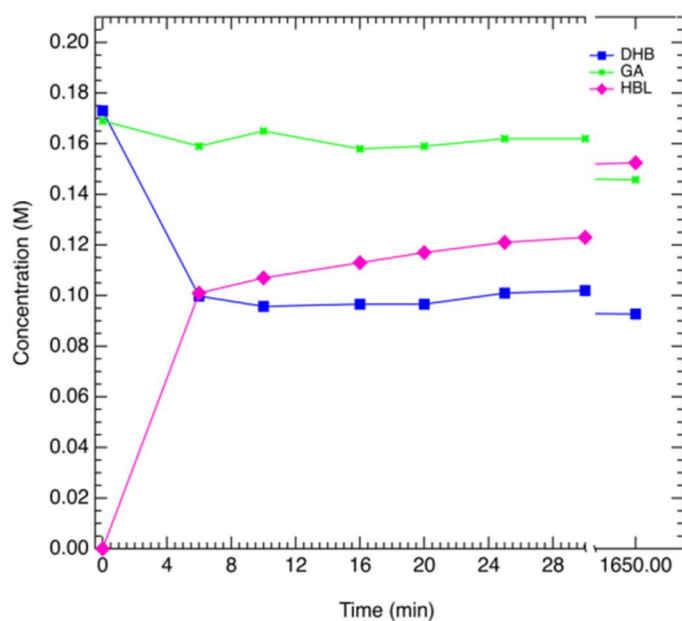


Figure 21. Estimated product distribution of acid catalyzed lactonization of DHB to HBL at reaction conditions: 330K, 0.156M trione, 0.3M piperazine, and 1.76M HCl (39).

## **Results & Discussion**

As previously mentioned, the outcomes of this process have proven difficult to quantify. There is uncertainty surrounding the intermediate steps. Beginning with 0.55 M glucose, we do arrive at 0.55 M glucosone (35). From there, quantification of outcomes has proven more difficult. While we can confirm the presence of the intermediate trione through the use of H-NMR and  $^{13}\text{C}$ -NMR, quantification is limited by the peak overlap among equilibrated anomers and potential byproducts and impurities in the supernatant (34). This is further complicated by the addition of the homogeneous base and acid catalysts which facilitate the known production of byproducts, namely polyols and glycolic acid (GA). Despite these limitations, kinetic modeling based on known quantities did prove accurate enough to make assumptions as to outcomes for further analysis (36). These results were used as the basis of continuing research in extracting the HBL from solution and performing a techno-economic analysis to determine the financial viability of the proposed synthesis.

### Chapter 3

#### CHIRALITY OF SYNTHESIZED HBL

Having proven the concept we sought to better quantify the outcomes. Crucial to the synthesis is the enantiomeric purity of the resulting HBL. With the only difference between the (R) and (S) enantiomers being the mirrored structure centered around its singular chiral carbon, in any synthesis this becomes difficult to discern.

#### Materials & Methods

NMR analysis proved HBL synthesis, but does not provide resolution to prove chirality. To resolve this, the product resulting from the outlined pathway was evaluated using gas chromatography (GC) with flame ionization detection (FID). This was done with instrumentation outlined in a 2008 research paper on HBL synthesis which used the MilliporeSigma™ Supelco™  $\beta$ -Dex 255 capillary GC column containing a chiral stationary phase of 2,3-diO-acetyl-6-O-TBDMS- $\beta$ -cyclodextrin. (43) This column successfully separated aqueous and organic solutions of R and S HBL with retention times heavily dependent on the extraction solvent. This provided a good basis against which to compare synthesized HBL after extracting it from the reaction solution. For GC experiments we used helium carrier gas, inlet temp. 250 °C, column temp. 205 °C, FID temp 300 °C, and continuous flow of 1ml/min.





*Figure 22. Agilent 7820A Gas Chromatography System*

Prior to selecting this column for experimentation, several attempts were made to obtain peak resolution using high performance liquid chromatography (HPLC) to no avail. Initial trials were run using the Lux™ Amylose-3™ column with amylose tris(3-cholor-5-methylphenylcarbamate) as the chiral selector. While this column could identify the presence of both S and R HBL, there was no discernible difference between the retention times. These tests were performed using a variety of both aqueous and organic mobile phases. In collaboration with Phenologix™ additional HPLC columns were tested to include: Lux™ Cellulose-1™, Lux™ Cellulose-2™, Lux™ Cellulose-3™, Lux™ Cellulose-4™, Lux™ Amylose-2™. These were all tested, as with the previous column, using a variety of mobile phases. None proved capable of distinguishing the two enantiomers.

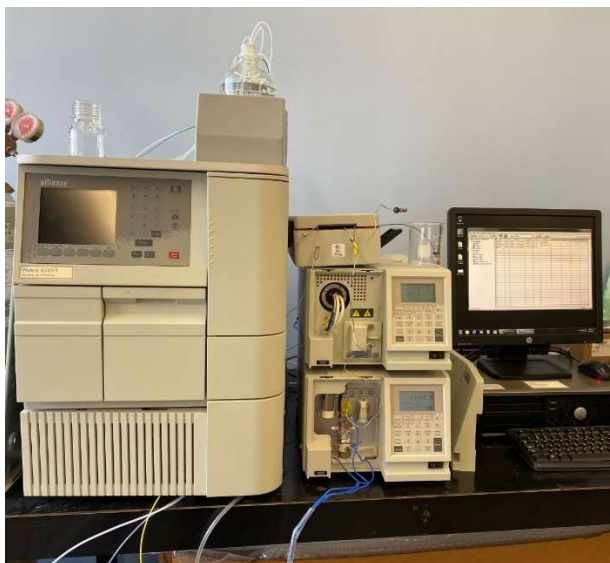


*Figure 23. Waters e2695 HPLC System*

H-NMR and  $^{13}\text{C}$ -NMR analysis was also performed on racemic solutions to compare against HBL extracted from reaction solution. NMR analysis was conducted on the Inova 400 with D<sub>2</sub>O added for signal lock. Spectrometer frequency was set to 100.569 MHz, at 5.750  $\mu\text{s}$  pulse width, 1.303 s acquisition time, and 2000 for number of transients.



*Figure 24. Inova 400 NMR System*

## Divergence Of Chiral Peaks

Analysis of the broader reaction network from glucose to HBL suggests that chirality has been preserved in the critical C-5 carbon as noted in the figure below.

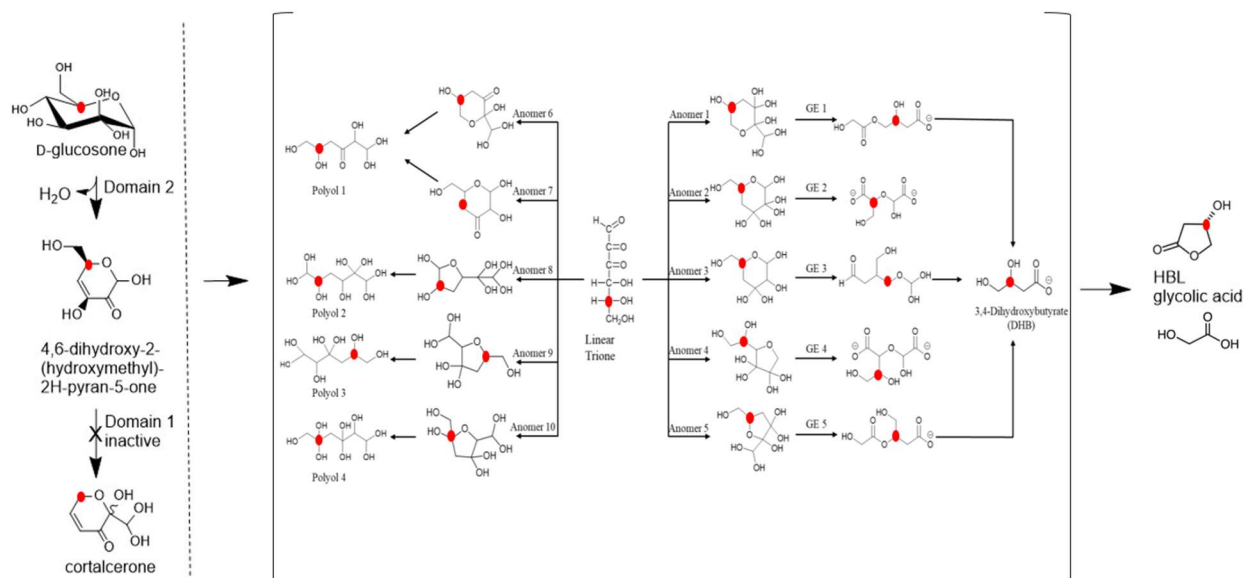
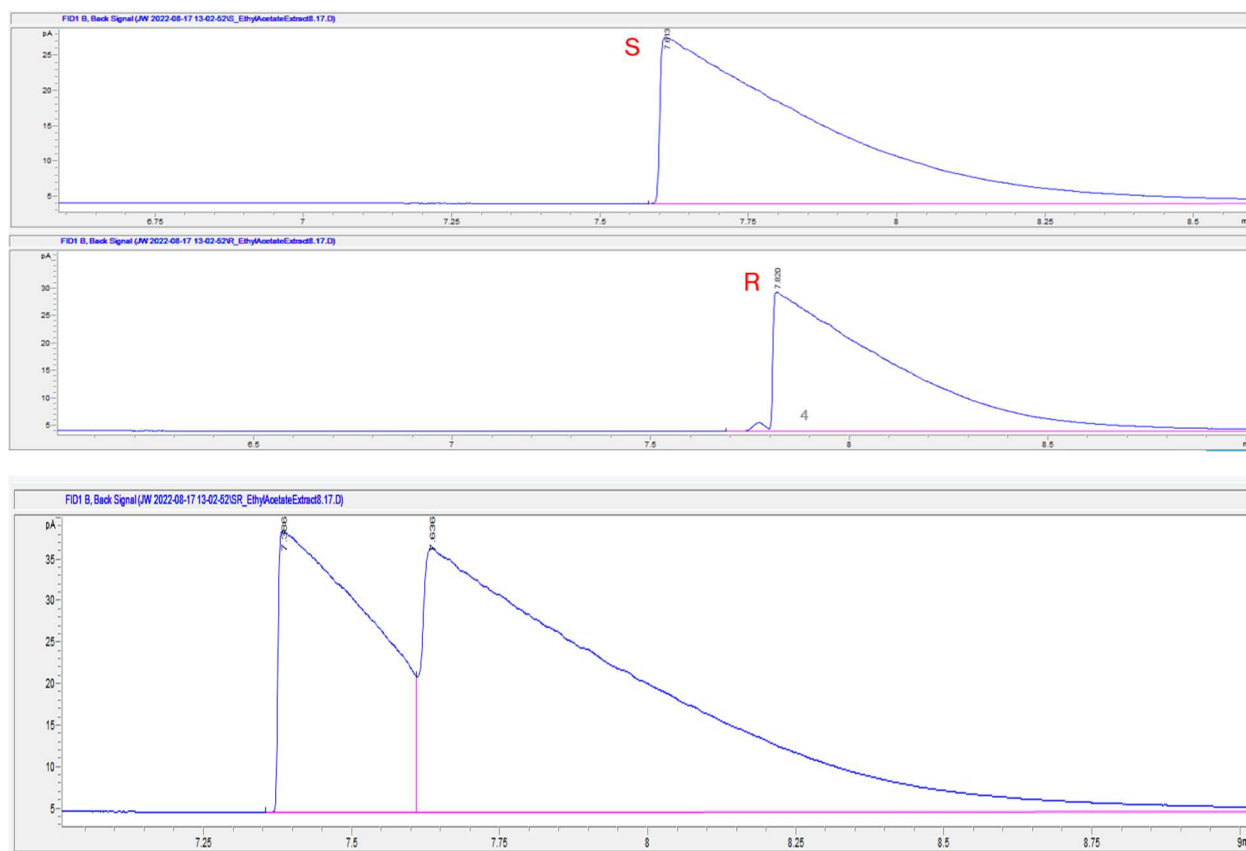


*Figure 25. Reaction network of enzyme and chemical catalyzed HBL synthesis with highlight of conserved chirality.*

To examine this experimentally, we used a strategy of “dosing” in which a sample of HBL extracted from the reaction solution was evaluated using gas chromatography to identify the corresponding HBL peak. Once the HBL peak was identified, additional samples were then dosed with a solution of HBL containing pure standards of each enantiomer of HBL at equal concentrations. The resulting divergence in peaks with the (R)-dosed sample and the lack of peak divergence in the (S)-dosed sample confirmed our theorized outcome; the synthesis outlined in this paper produces enantiomerically pure HBL.

(a)



(b)

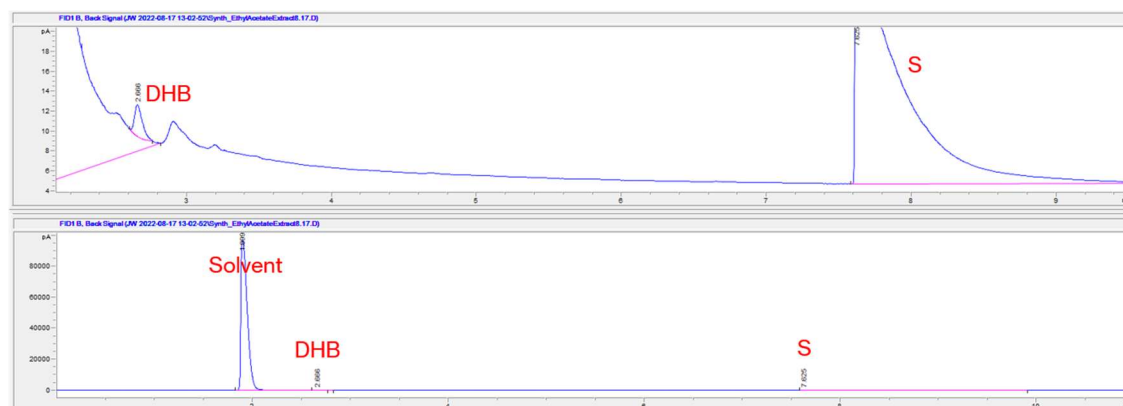


Figure 26. Gas chromatography with flame ionization detection (GC-FID) analysis of HBL enantiomers. Method for analysis included; helium carrier gas, inlet temperature 250 °C, column temperature 205 °C, FID temperature 300 °C, flow of 1ml/min. (a) S and R HBL pure standards extracted from aqueous solution into ethyl acetate. (b) Reaction sample extracted from aqueous solution into ethyl acetate zoomed in (top) and with full chromatograph (bottom).

## **Results & Discussion**

The combination of GC-FID analysis and close investigation of the broader reaction network strongly suggests an enantiomerically pure synthesis. However, there is the possibility that some minute quantity of R-HBL could be in solution and that the GC analysis lacks the resolution to distinguish between this negligible concentration of R-HBL given that there is some peak overlap where the detection for the undesired enantiomer could be masked. While unlikely, this cannot be ruled out without further experimentation.

## Chapter 4

### LIQUID-LIQUID EXTRACTION

Identifying an extraction solvent for experimentation proved difficult as the a-symmetrical, polar, cyclic, HBL molecule has greater affinity for polar solvents like water. A number of organic solvents were tested for extraction of HBL from the aqueous phase with many failing to dissolve HBL in any meaningful concentration. Of those tested, ethyl acetate (EA), propylene carbonate (PC), and tetrahydrofuran (THF) showed the greatest promise in terms of both immiscibility and their ability to dissolve HBL. Calibration curves for HBL solutions of each of the organic solvents and for aqueous solutions were generated against the MilliporeSigma™ Supelco™ β-Dex 255 capillary GC column (see Appendix).

Partition coefficients (kp) for each solvent were evaluated. To obtain this value, these solvents were tested for their ability to extract HBL from aqueous solution at varying concentrations with the Kp value being the resulting ratio of HBL concentration between the aqueous and organic phases. Values were calculated based on experimentation at ambient conditions.

$$Kp = \frac{\left[\frac{g}{ml}\right]_{organic}}{\left[\frac{g}{ml}\right]_{aqueous}}$$

*Equation 3. Partition coefficient defined as the ratio of organic and aqueous solution concentrations in g/ml.*

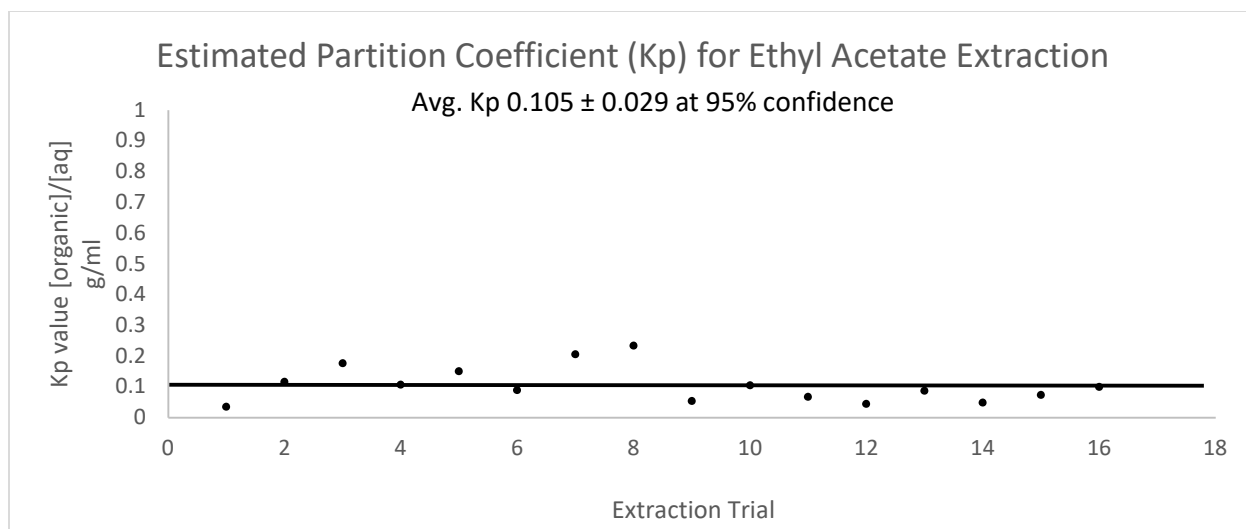


Figure 27. Calculated partition coefficient for ethyl acetate extraction of HBL in aqueous solution.

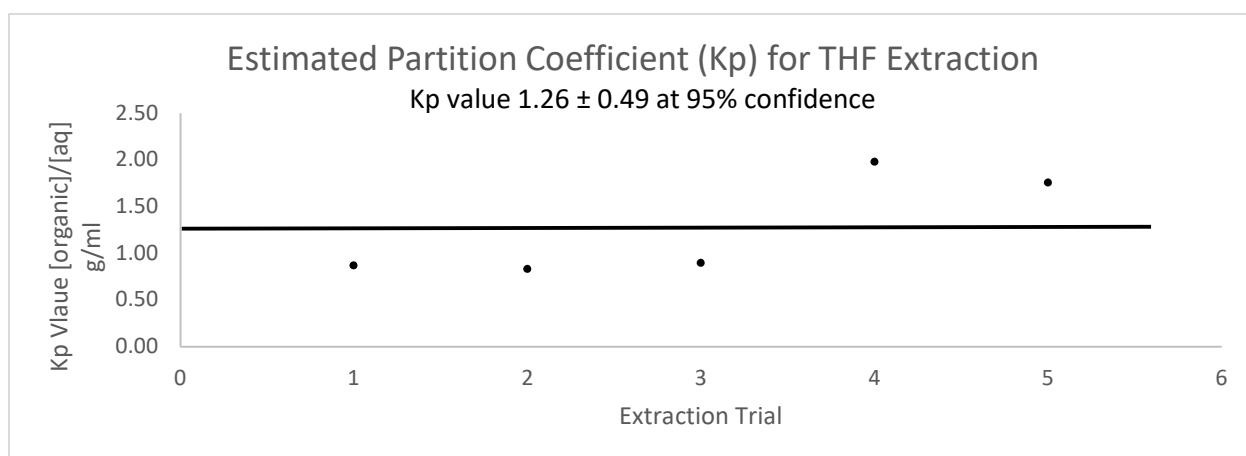


Figure 28. Calculated partition coefficient for THF extraction of HBL in aqueous solution.

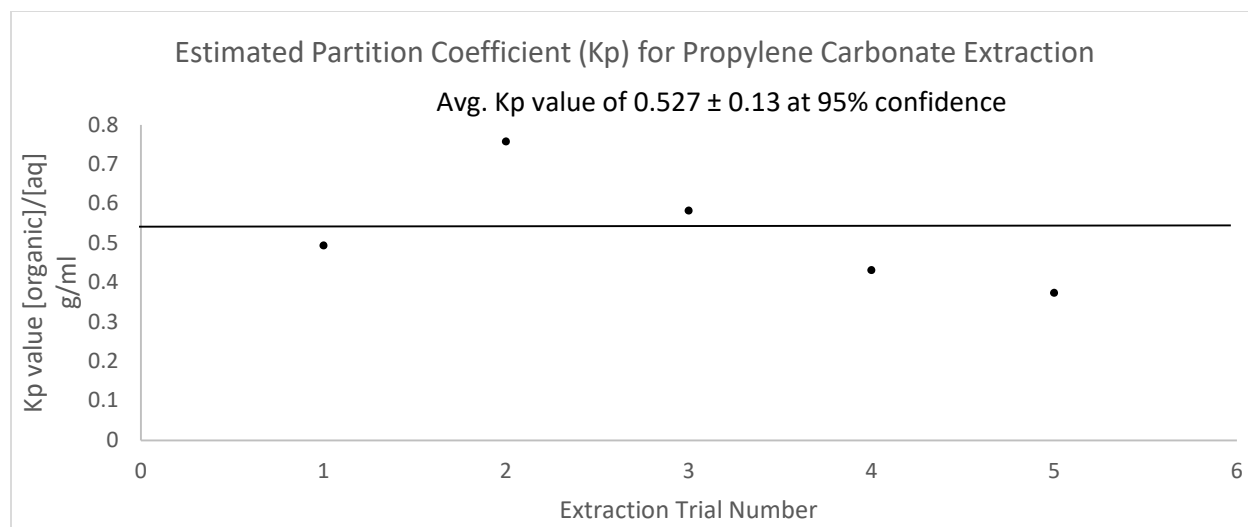


Figure 29. Calculated partition coefficient for propylene carbonate extraction of HBL in aqueous solution.

Despite THF having a better partition coefficient than ethyl acetate and propylene carbonate, and thus a greater ability to extract HBL; for experimentation, ethyl acetate was chosen because the resulting chromatographs showed no contaminants. Of the three solvents, ethyl acetate appears more selective in its ability to extract HBL from the aqueous solution (comparative example in appendix). Attempts were made to measure the impact of adding salts to the aqueous phase of the liquid-liquid extraction; however, no notable increase in HBL concentrations was noted in the organic phase.

Batch reactions were agitated in the presence of ethyl acetate, and extractions performed using a separatory funnel after 24hrs rest time. Extraction and analysis using calculated  $K_p$  values of batch syntheses showed a resulting concentration in agreement with prior NMR analysis estimates of 0.14 M. Error bars on the extraction points account for the upper and lower



bounds of ethyl acetate Kp values.

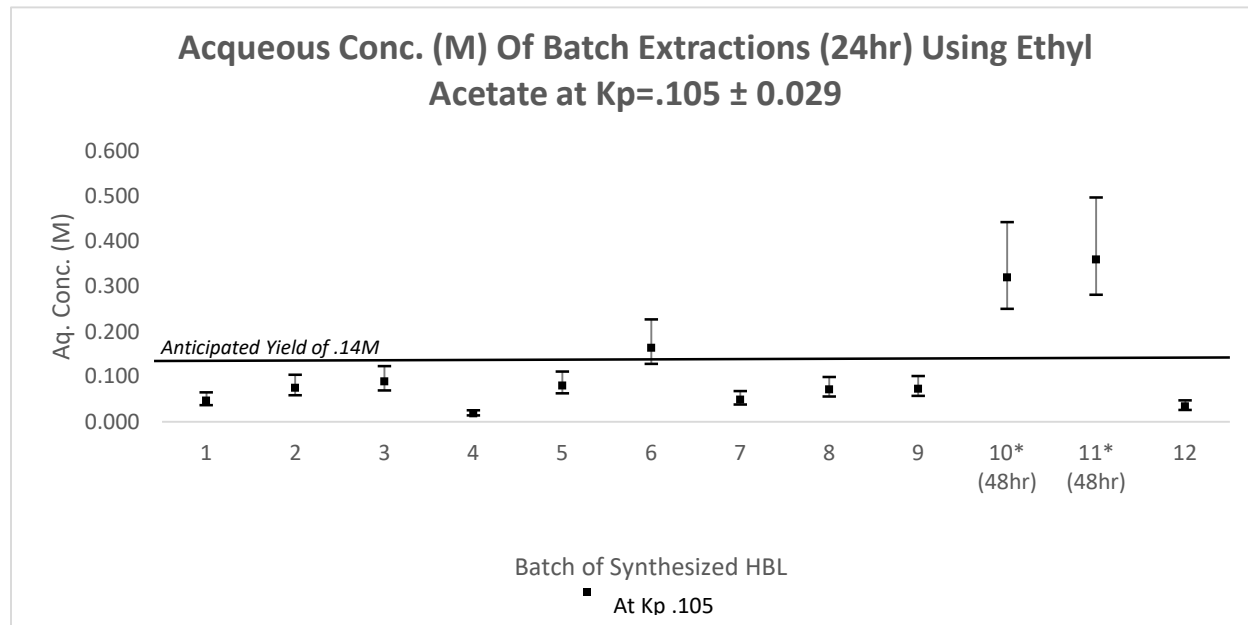


*Figure 30. Concentration of HBL synthesized in aqueous phase based on calculated  $K_p$  values and ethyl acetate extraction concentrations after 24hrs.*

In two instances, the rest time extended to 48 hours and showed an increased concentration of HBL after GC-FID analysis. This suggests that the equilibrium-limited aqueous reaction shifts towards HBL as it is extracted into the organic phase. This, as previously mentioned, suggests improved HBL recovery in industrial applications with the use of a biphasic reactor.

Synthesis was done using two distinct batches of trione. Each batch was prepared in the manner outlined in chapter 2; however, the outcome was visually different with trione from batch 707-103 considerably darker in color (yellowish) when compared to trione from batch 707-112 as can be seen in the image below. To determine whether this color difference impacted chemical catalysis, comparisons were made between experiments run with each. In the HBL synthesis graph above, batches 1 thru 6 and batch 12 were run using trione from 707-

103. Batches 7 thru 11 were run using trione from 707-112. With the exception of the instances in which extractions ran for longer than 24 hours, thus shifting the equilibrium towards greater HBL production, there was no notable difference between the two batches. Visual differences between the trione batches did not translate into differences in HBL synthesis outcomes. Biogenic impurities are the likely cause of these impurities as whole cell catalysis can result in degradation of cell walls; however, if this is the case, trione concentrations and subsequent chemical catalysis do not appear to be impacted (34).



*Figure 31. Trione from batches 707-103 (left), and batches 707-112 (right). There are notable color differences; however, they do not appear to impact HBL synthesis.*

### **Materials & Methods**

Extractions were performed using equal volumes of aqueous reaction solution and ethyl acetate at ambient temperature and atmospheric pressures. Each biphasic mixture was agitated in a sealed flask for 20 minutes using the Ohaus™ SHRC0719DG reciprocating shaker at 20 rotations per minute. The mixtures were then transferred to separatory funnels (pictured below) and allowed to rest for 24 hours to reach equilibrium. After the allotted time, organic

and aqueous phases were separated and GC analysis using previously noted columns and methods was performed. Based on measured  $k_p$  values and established standard curves, aqueous and organic phase HBL concentrations for each batch were calculated.



*Figure 32. Separatory funnels used in liquid-liquid HBL extraction. Organic phase (top) and aqueous phase (bottom).*

### **Results & Discussion**

The data obtained from extraction experiments reveal a key insight that can be exploited for industrial scale production. GC-FID analysis suggests ethyl acetate is a more selective extraction solvent as it appears only to remove HBL from solution and not the glycolic acid, polyols, piperazine, and other byproducts and reactants from within the broader network. This makes it an easy choice when scaling up as less refinement is required. Moreover, ethyl acetate is also a very volatile solvent, with a boiling point much lower than that of water or HBL at 77 C, 100 C, and 100 C respectively. This makes it ideal for distilling HBL in downstream processing as will be discussed in the following chapter.

## Chapter 5

### TECHNO-ECONOMIC ANALYSIS

Preliminary techno-economic analysis (TEA) was conducted to determine the economic viability of this synthesis following the discounted cash flow method (DCF). This type of financial model evaluates the value of an investment based on future cash flows (48).

$$DCF = \frac{CF_1}{(1+r)^1} + \frac{CF_2}{(1+r)^2} + \frac{CF_n}{(1+r)^n}$$

*Equation 4. Discounted cash flow (DCF) is equal to the sum of the cash flows 'CF' for each period 'n' divided by 1+ r, with 'r' equivalent to the devaluation rate.*

The annual production capacity of 120 metric-tonnes was selected as a benchmark against a plant in South Korea, SK Energy & Chemical, which has produced this amount annually since its opening in 2003. The HBL made by this plant is produced through the hydrogenation of esters of L-malic acid and sells wholesale for \$450/kg (6).

### Materials & Methods

A process flow diagram was created to produce HBL with a high purity (>99.9%) from glucose, beginning with the whole cell catalysis and proceeding through to extraction and distillation of the final product. Leidos™ hanging bag reactors were selected for conversion of glucosone to trione via whole cell enzyme catalysis. They were selected due to their relative low-cost, the ease of replacing and cleaning, and their proven track record for biochemical synthesis with

sparging of reactant gases. The volume of these reactors were determined using the residence time and the glucose mass flow rates (45) (46). The remaining homogeneous chemical catalysis stages and HBL extraction were modeled using Aspen Plus™ process simulation software (47). State-of-the-art process equipment was selected for the homogeneous chemical catalysis stages and the HBL extraction. The process equipment was sized using the simulated material and energy balances, with all reactions simulated at 25 C and 1 atm. The size of the process equipment was used as a basis to assess the capital costs, and the material and energy balances were used to calculate the operating costs (48).

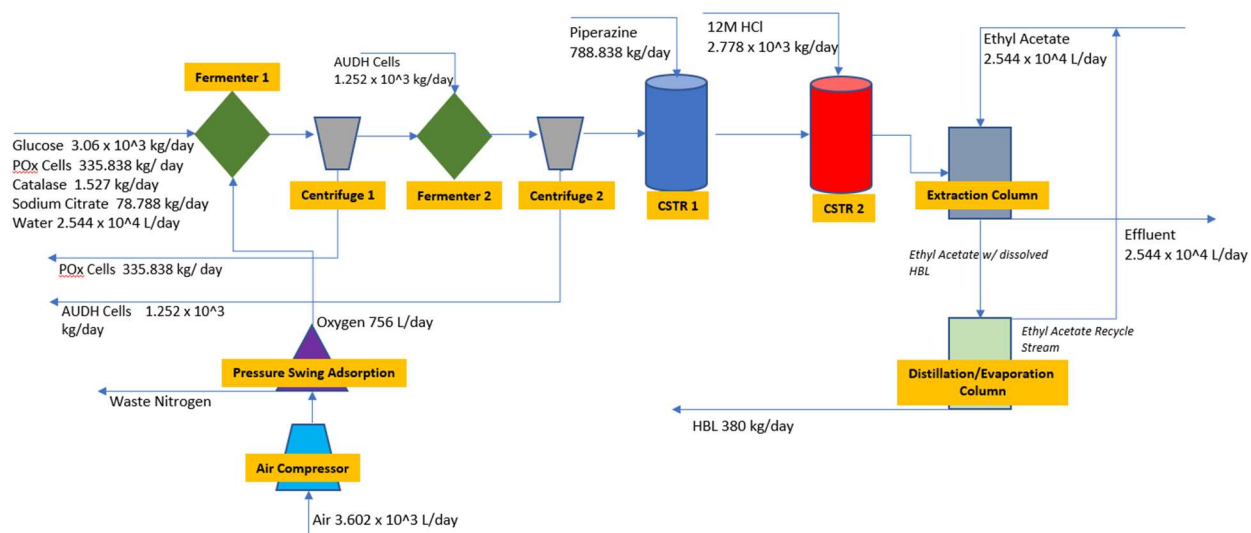


Figure 33. Process flow diagram for the production of HBL from glucose at 380kg/day production.

The seed trains are used to make POx and AUDH cells. This process takes cryogenically frozen cells and grows them with the proper nutrients in successively larger culture vessels until the desired volume is reached. These cells are placed into the hanging bag fermenters in an aqueous glucose solution to ultimately form trione. Oxygen used in sparging for these stages is

produced from air compressed to 7 bar and processed using the pressure swing adsorption. After the biocatalyzed conversions of glucose and glucosone, the cells are recovered for reuse using the centrifuge. The resulting trione solution is passed through two successive CSTRs for the base and acid catalyzed reactions. The HBL from these reactions is extracted by ethyl acetate from the product mixture using two solvent extraction columns. The first solvent extraction column is operated at 25 C and 1 atm with 12 stages. In the first extraction column, the solvent to feed ratio (on a mass basis) is maintained at 10:1. The raffinate from the first extraction column is sent to a second solvent extraction column for further recovery of HBL. Testing of the Aspen model showed that for the second extraction column, 8 stages, a temperature of 25 C, a pressure of 1 atm., and a solvent to feed ratio of 10 was found to be optimal for HBL extraction. About 95% of the produced HBL can be extracted into ethyl acetate using the two solvent extraction columns. The extracts from both solvent extraction columns are routed to a distillation column to recover ethyl acetate as a distillate for reuse. The bottoms from the distillation column are sent to a vacuum evaporator to produce HBL as a liquid product with a purity of greater than 99.5%. The ethyl acetate vapors from the vacuum evaporator are also condensed for reuse.

### **Results & Discussion**

The capital and the annual operating costs to produce HBL at the selected scale were determined at \$32.6 MM and \$15.9 MM, respectively. At scale, the TEA analysis predicts the minimum selling price of HBL is \$165 per kg, this is 63% less than what is currently available

(14). Evidence suggests this pathway to the production of enantiomerically pure HBL is not only more chemically favorable than existing methods, but also more financially favorable. Should this method be implemented, the reduced production costs could have numerous downstream benefits for drug manufacturers and ultimately for consumers.

## Chapter 6

### **CONCLUSION & OUTLOOK**

This thesis reviewed the importance of HBL as a chiral building block for pharmaceutical synthesis and current methods for industrial scale synthesis as well as related costs and impacts, highlighting the need for improvements on petrochemical derivations. Over the course of the research project, a number of biological and chemical routes to HBL synthesis were explored, but none proved capable of reaching industrial scale with efficiencies rivaling current production. A newly proposed route combining biological and chemical catalysis was proposed through which low-cost bioderived glucose feedstocks could be used to produce chiral HBL at scale. Experimentation and modeling suggest that this method is viable and could potentially reduce the cost of manufacturing by more than 50%. This economically and environmentally favorable option presents exciting opportunities not only for HBL production and cost reduction, but also for the countless downstream applications. Realization of these methods could reduce the cost of pharmaceuticals, a much-needed salve to exploding U.S. healthcare costs.

### **Recommendations for Future Work**

There are a few areas highlighted over the course of this work that could benefit from deeper exploration in the future. Beginning with the biological processes; this process uses whole cell catalysis. This eliminates the need for enzyme purifications since they are contained within the cells; however, it exposes the process to a potential flaw. The cells used are washed, frozen, and reused in subsequent syntheses. As the enzyme catalyzed stages require thorough mixing,



these cells, and specifically their cell walls, are prone to degradation over time. The contents of these cells would then leak into the reaction solution, and critical enzymes would be lost in subsequent washes, potentially degrading production over time. While the impurities of the cell contents may not negatively impact HBL synthesis as is implied by the negligible differences between the visually contrasting trione batches, the loss of POx and AUDH enzymes contained within would negatively impact HBL synthesis. Thus, this research could benefit from exploration of methods to immobilize the whole cells used in catalysis. This would reduce cell wall degradation, and longevity in cell reusability.

The research could further benefit from improved observations of chirality. Efforts to quantify chirality using a Jasco model DIP-370 digital polarimeter were inconclusive due to instrument failure. Though evidence strongly suggests chirality, for the purity required of pharmaceutical applications, this must be more thoroughly verified.

## REFERENCES

1. **Aitken, M., Kleinrock, M. and Munoz, E.** IQVIA. *Global Medicine Spending And Usage Trends: Outlook To 2025*. [Online] 2021. <https://www.iqvia.com/insights/the-iqvia-institute/reports/global-medicine-spending-and-usage-trends-outlook-to-2025>.
2. **Langreth, R.** Quick Take: Drug Prices. *Bloomberg*. September 16, 2020.
3. *The God In The Machine*. **Lapham, L.** 2009, Lapham's Quarterly, Medicine 2(4).
4. **Bozell, J. J. and Petersen, G. R.** Technology Development For The Production Of Biobased Products From Biorefinery Carbohydrates - The US Department Of Energy's "Top 10" Revisited. *Green Chemistry*. 2010, 12, pp. 539-555.
5. **Werpy, T. and Peterson, G.** *Top Value Added Chemicals From Biomass: Volume I--Results of Screening for Potential Candidates from Sugars and Synthesis Gas*. s.l. : Department of Energy, 2004. GO-102004-101992.
6. *Custom Chemicals*. **Rouhi, A. M.** s.l. : Chemical Engineering News, 2003, Vol. 81, pp. 55-73.
7. *A Platform Pathway For Production Of 3-Hydroxyacids Provides A Biosynthetic Route To 3-Hydroxy-Gamma-Butyrolactone*. **Martin, Colin H., et al.** 1414, s.l. : Nature Communications, 2012, Vol. 4.
8. *A Simple And Practical Approach To Enantiomerically Pure (S)-3-Hydroxy-Gamma-Butyrolactone: Synthesis Of (R)-4-Cyano-3-Hydroxybutyric Acid Ethyl Ester*. **Kumar, P., et al.** 2005, Tetrahedron Asymmetry, Vol. 16, pp. 2717-2721.
9. *Crystal Structure Of HIV-1 Protease In Complex With VX-478, A Potent And Orally Bioavailable Inhibitor Of The Enzyme*. **Kim, E. E. and et al.** . 1995, American Chemical Society, Vol. 117, pp. 1181-1182.
10. *Synthetic Routes To L-Carnitine And L-Gamma-Amino-Betahydroxybutyric Acid From (S)-3-Hydroxybutyrolactone By Functional Group Priority Switching*. . **Wang, G. and Hollingsworth, R. I.** . 1999, Tetrahedron Asymmetry, Vol. 10, pp. 1895-1901.
11. **ChemicalBook**. Chemicalbook.com. *CAS Database List (S)-3-Hydroxy-gamma-butyrolactone*. [Online] ChemicalBook. [Cited: March 23, 2023.] [https://www.chemicalbook.com/ChemicalProductProperty\\_EN\\_CB6360496.htm](https://www.chemicalbook.com/ChemicalProductProperty_EN_CB6360496.htm).
12. *Uses and Production of Chiral 3-Hydroxy-Gamma-Butyrolactones and Structurally Related Chemicals*. **Lee, Sang-Hyun and Park, Oh-Jin.** 84, s.l. : Applied Microbiology and Biotechnology, 2009, pp. 817-828.
13. **Mikulic, M.** Pfizer's Lipitor Revenue Worldwide 2003-2019. *Statista*. [Online] July 27, 2022. [Cited: March 23, 2023.] <https://www.statista.com/statistics/254341/pfizers-worldwide-viagra-revenues-since-2003/>.
14. *A Platform Pathway For Production Of 3-Hydroxyacids Provides A Biosynthetic Route To 3-Hydroxy-Gamma-Butyrolactone*. **Martin, C., et al.** 2013, Nature Communications, (4)1414.

15. *Toward A Carbohydrate-Based Chemistry: Progress In The Development of General-Purpose Chiral Synthons From Carbohydrates.* **Hollingsworth , R. I. and Wang, G.** 2000, Chemical Reviews, Vol. 100, pp. 4267-4282.
16. **Chun, Jongpil, et al.** *Process For Preparing Optically Pure (S)-3-Hydroxy-Gamma-Butyrolactone.* 6124122 United States , July 23, 1999.
17. *Continuous Process for the Production of Optically Pure (S)-beta-hydroxy-gamma-butyrolactone.* **Kwak, B. S., et al.** 2006.
18. *A Revised Mechanism for Chemoselective Reduction of Esters With Borane-Dimethyl Sulfide Complex and Catalytic Sodium Tetrahydroborate Directed by Adjacent Hydroxyl Group.* **Saito, S., et al.** s.l. : Tetrahedron, 1999, Vol. 48, pp. 4067-4086.
19. *Synthesis of homochiral tetrahydropteridines.* **Baker, S. J., Beresford, K J. M. and Young, D. W.** s.l. : Tetrahedron, 2014, Vol. 70, pp. 7221-7228.
20. **Blair, G. T. and DeFraties, J. J.** *Hydroxy Dicarboxylic Acids.* s.l. : Kirk-Othmer Encyclopedia of Chemical Technology, John Wiley & Sons Inc., 2000.
21. **Felthouse, T. R., et al.** *Maleic Anhydride, MAleic Acid, and Fumaric Acid.* s.l. : Kirk-Othmer Encyclopedia of Chemical Technology, John Wiley & Sons, 2000.
22. *Inhibition of Metal Hydrogenation Catalysts by Biogenic Impurities.* **Schwartz, T. J., Brentzel, Z. J. and Dumesic, J. A.** s.l. : Catalysis Letters, 2015, Vol. 145, pp. 15-22.
23. *Engineering Catalyst Microenvironments for Metal-Catalyzed Hydrogenation of Biologically-Derived Platform Chemicals.* **Schwartz, T. J., et al.** s.l. : Angewandte Chemie Internaitonal Edition, 2014, Vol. 53, pp. 12718-12722.
24. **Hollingsworth, Rawle I.** *Process for the Preparation of Hydroxy Substituted Gamma Butyrolactones .* PCT/US98/20448 United States , September 29, 1998. Application.
25. *Microbial biosynthesis and secretion of l-malic acid and its applications.* **Chi, Z., et al.** s.l. : Critical Reviews in Biotechnology, 2016, Vol. 36, pp. 99-107.
26. *Coupling Chemical And Biological Catalysis: A Flecible Paradigm for Producing Biobased Chemicals.* **Schwartz, T. J., Shanks, B. H. and Dumesic, J. A.** s.l. : Current Opinion In Biotechnology, 2016, Vol. 38, pp. 54-62.
27. *Integration of Chemcial and Biological Catalysis: Production of Furyglycolic Acid from Glucose via Cortalcerone.* **Schwartz, T. J. and al., et.** s.l. : ACS Catalysis, 2013, Vol. 3, pp. 2689-2693.
28. *Pyranose oxidase and pyranosone dehydratase enzymes responsible for conversion of D-glucose to cortalcerone by the basidiomycete phanerochaete chrysosporium.* **Volc, J., et al.** s.l. : Archives of Microbiology, 1991, Vol. 156, pp. 297-301.
29. *Bridging the Chemical and Biological Catalysis Gap: Challenges and Outlooks for Producing Sustainable Chemicals.* **Schwartz, T. J., et al.** s.l. : ACS Catalysis, 2014, Vol. 4, pp. 2060-2069.

30. *Inhibition of Metal Hydrogenation Catalysts by Biogenic Impurities*. **Schwarta, T. J., Brentzel, Z. J. and Dumesic, J. A.** s.l. : Catalysis, 2015, Vol. 145, pp. 15-22.
31. *Single-reactor process for sequential aldol-condensation and hydrogenation of biomass-derived compounds in water*. **Barrett, C. J., et al.** s.l. : Applied Catalysis B: Environmental, 2006, Vol. 66, pp. 111-118.
32. *Engineering E. coli for the biosynthesis of 3-hydroxy-gamma-butyrolactone (3HBL) and 3,4-dihydroxybutyric acid (3,4-DHBA) as value-added chemicals from glucose as a sole carbon source*. **Dhamankar, H., et al.** s.l. : Metabolic Engineering, 2014, Vol. 25, pp. 72-81.
33. *Integration of Chemical and Biological Catalysis: Production of Furyglycolic Acid from Glucose via Cortalcerone*. **Schwartz, T. J., et al.** s.l. : ACS Catalysis, 2013, Vol. 3, pp. 2689-2693.
34. **Kersten, P. J. and Schwartz, T. J.** *Study Plan: High-Value Chemicals (3-hydroxybutyrolactone) from Wood*. Orono : FPL/University of Maine Agreement, 2018. 18-JV-1111126-045.
35. *Repurposing Inflatable Packaging Pillows as Bioreactors: A Convenient Synthesis of Glucosone by Whole-Cell Catalysis under Oxygen*. **Mozuch, M. D., et al.** s.l. : Applied Biochemistry And Biotechnology, 2021, Vol. 193, pp. 743-760.
36. **Jamalzade, Elnaz.** *New Catalytic Routes For Upgrading Biomass-Derived Organic Molecules*. Chemical Engineering , University of Maine . Orono : University of Maine Graduate School, 2021. Dissertation.
37. **Abdulrazzaq, H. T.** *Reaction Kinetics and Mechanism Investigations of Renewable Chemicals Production from Woody Biomass* . s.l. : University of Maine (Thesis), 2020.
38. **Frisch, M. J., et al.** *No Title*. 2016.
39. **Boudart, M.** *Turnover Rates in Heterogeneous Catalysis*. 1995. pp. 661-666.
40. **Carey, F. A.** *Organic Chemistry. Chimia Vol. 65*. s.l. : McGraw Hill, 2000.
41. *Acid-Base Pairs in LEwis Acidic Zeolites Promote Direct Aldol Reactions by Soft Enolization,*. **Lewis, J. D., Van de Vyver, S. and Roman-Leshkov, Y.** s.l. : Angewandte Chemie International, 2015, Vol. 54, pp. 9835-9838.
42. *Sustainable Production of Furfural in Biphasic Reactors Using Terpenoids and Hydrophobic Eutectic Solvents*. **Canada-Barcala, A., et al.** 30, Madrid : ACS Sustainable Chemical Engineering, 2021, Vol. 9, pp. 10266-10275.
43. **Lee, S. H., Park, O. J. and Uh, H. S.** *A Chemoenzymatic Approach To The Synthesis Of Enantiomerically Pure (S)-3-Hydroxy-Gamma-Butyrolactone*. *Appl. Microbiol. Biotechnol.* 2008, pp. 335-362.
44. **PubChem Compound Summary for CID 8028, Tetrahydrofuran.** s.l. : National Center for Biotechnology Information (2022), Retrieved December 12, 2022.

45. Clippinger, Jennifer and Davis, Ryan. *Techno-Economic Analysis for the Production of Algal Biomass via Closed Photobioreactors: Future Cost Potential Evaluated Across A Range of Cultivation Systems*. s.l. : National Renewable Energy Laboratory, 2019. NREL/TP-5100-72716.
46. Humbird, D., et al. *Process Design and Economics For Biochemical Conversion of Lignocellulosic Biomass to Ethanol*. Golden, Colorado : National REnewable Energy Laboratory, 2011. NREL/TP-5100-47764.
47. Inc., Aspen Technology. Aspen Plus . s.l. : AspenTech, 2019. Vol. Version 11.
48. R. , Turton, et al. *Analysis Synthesis and Design of Chemical Process*. Fifth Edition. s.l. : Pearson, 2018.

## APPENDIX

Homogenous Bases	Sodium Bicarbonate	Bis Tris Base	Tris Base	Piperazine
Conversion (%)	100	100	100	100
GE Maximum Yield (%)	91	98	37	23
Maximum Yield Time (hr)	23	21.5	2.5	1
DHB Yield (%)	0	0	14 <sup>b</sup>	100 <sup>c</sup>
GA Yield (%)	0	0	13.5 <sup>b</sup>	100 <sup>c</sup>
GE Yield after 23 hr	91	96	0	0
Trione consumption rate constant (1/min) <sup>a</sup>	0.05	0.07	0.06	0.14
Base Consumption (M)	0.065	0.11	0.298	0.28
Measured pH	8.45	9.39	10.36	11.41
pK <sub>b</sub>	7.6	7.5	5.9	4.2
Proton Affinity (kJ/mol)	920.3	928.1	972.4	979.2

<sup>a</sup>: Based on <sup>1</sup>H-NMR results. (b): Data collected after 19 hours. (c): Data collected after 22 hours

*Table 1. Results of treatment of trione solution with bases of varying proton affinity as calculated using DFT. The base with the greatest proton affinity, piperazine, achieved the highest yield of the intermediate chemical DHB (39).*

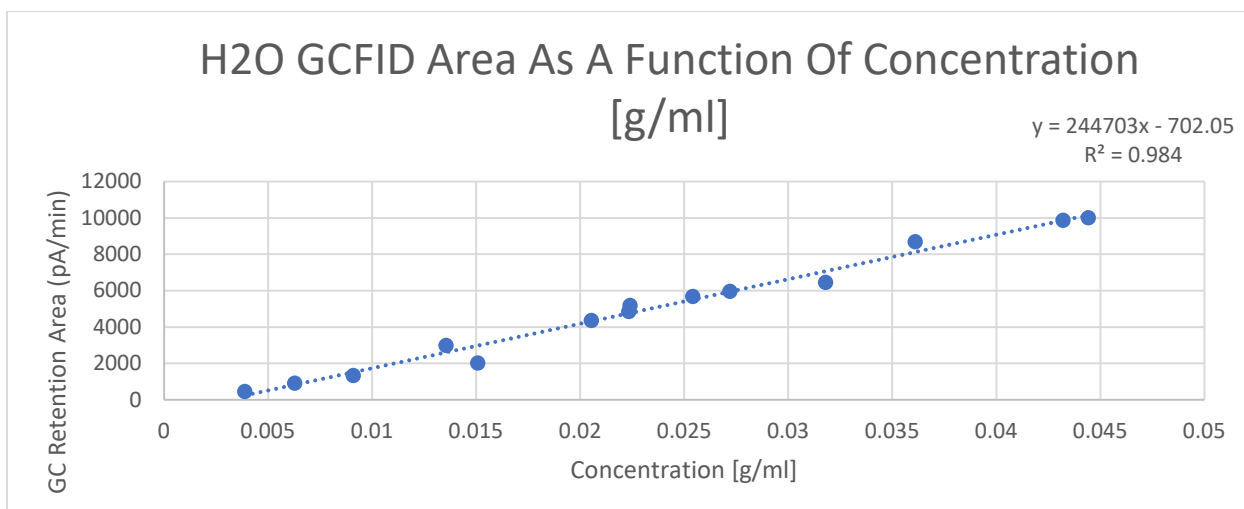


Figure 34. Standard curve for H2O MilliporeSigma™ Supelco™ β-Dex 255 capillary GC column containing a chiral stationary phase of 2,3-diO-acetyl-6-O-TBDMS-β-cyclodextrin. Helium carrier gas, inlet temp. 250 °C, column temp. 205 °C, FID temp 300 °C, and continuous flow of 1ml/min.

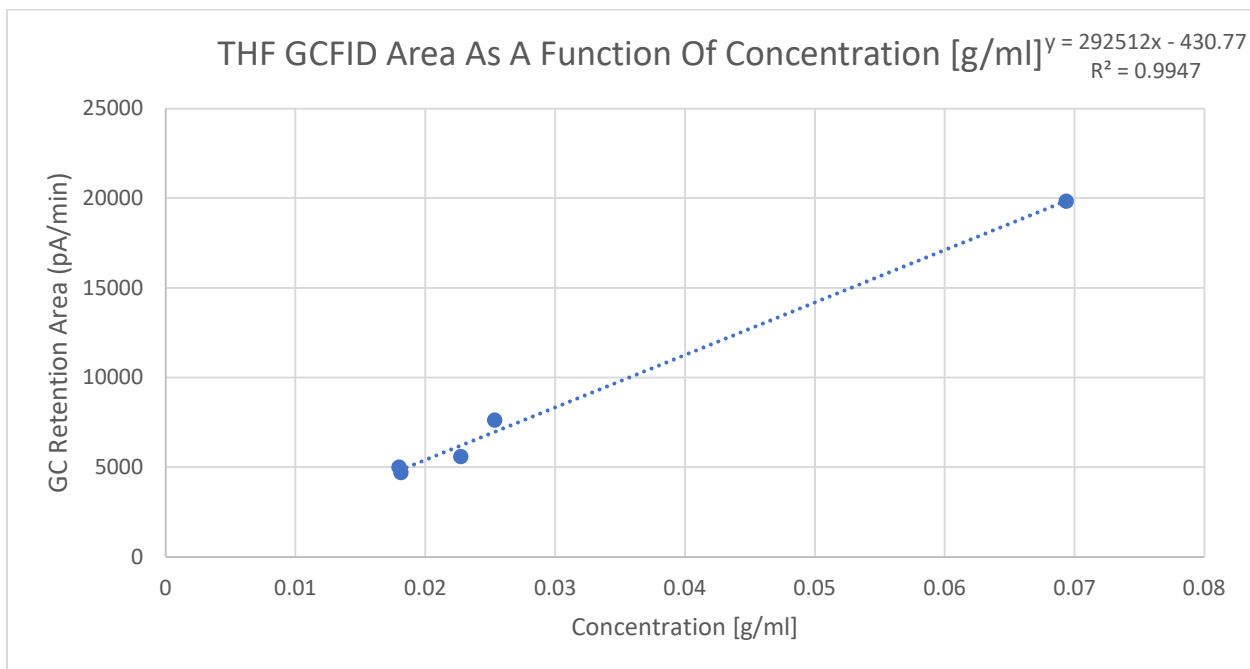


Figure 35. Standard curve for THF MilliporeSigma™ Supelco™ β-Dex 255 capillary GC column containing a chiral stationary phase of 2,3-diO-acetyl-6-O-TBDMS-β-cyclodextrin. Helium carrier gas, inlet temp. 250 °C, column temp. 205 °C, FID temp 300 °C, and continuous flow of 1ml/min.

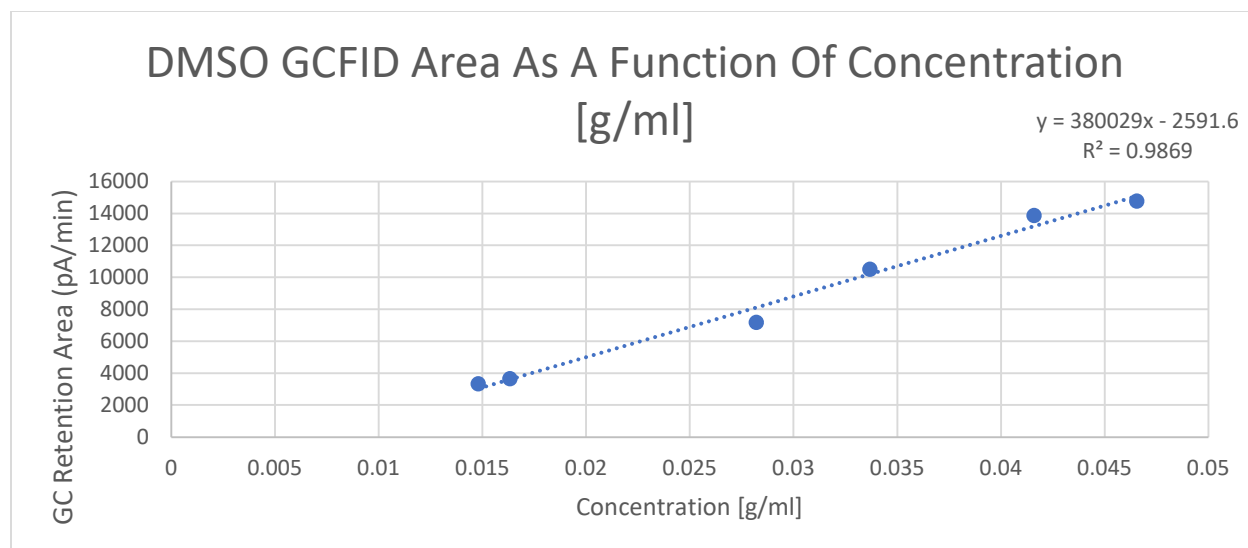


Figure 36. Standard curve for DMSO MilliporeSigma™ Supelco™ β-Dex 255 capillary GC column containing a chiral stationary phase of 2,3-diO-acetyl-6-O-TBDMS-β-cyclodextrin. Helium carrier gas, inlet temp. 250 °C, column temp. 205 °C, FID temp 300 °C, and continuous flow of 1ml/min.

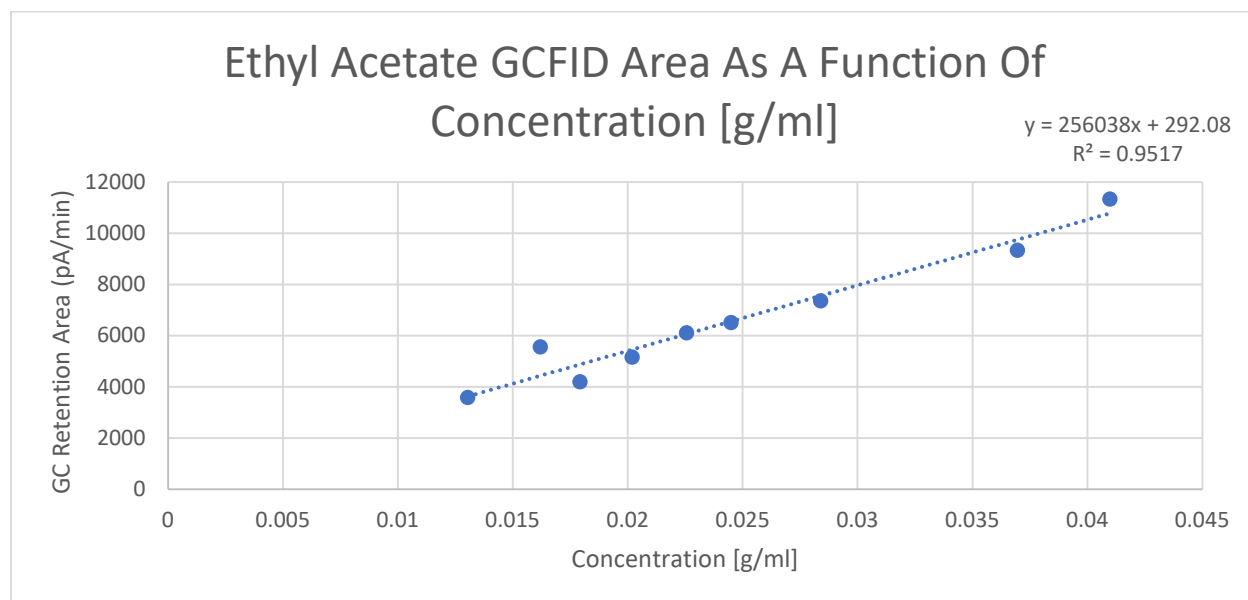


Figure 37. Standard curve for EA MilliporeSigma™ Supelco™ β-Dex 255 capillary GC column containing a chiral stationary phase of 2,3-diO-acetyl-6-O-TBDMS-β-cyclodextrin. Helium carrier gas, inlet temp. 250 °C, column temp. 205 °C, FID temp 300 °C, and continuous flow of 1ml/min.



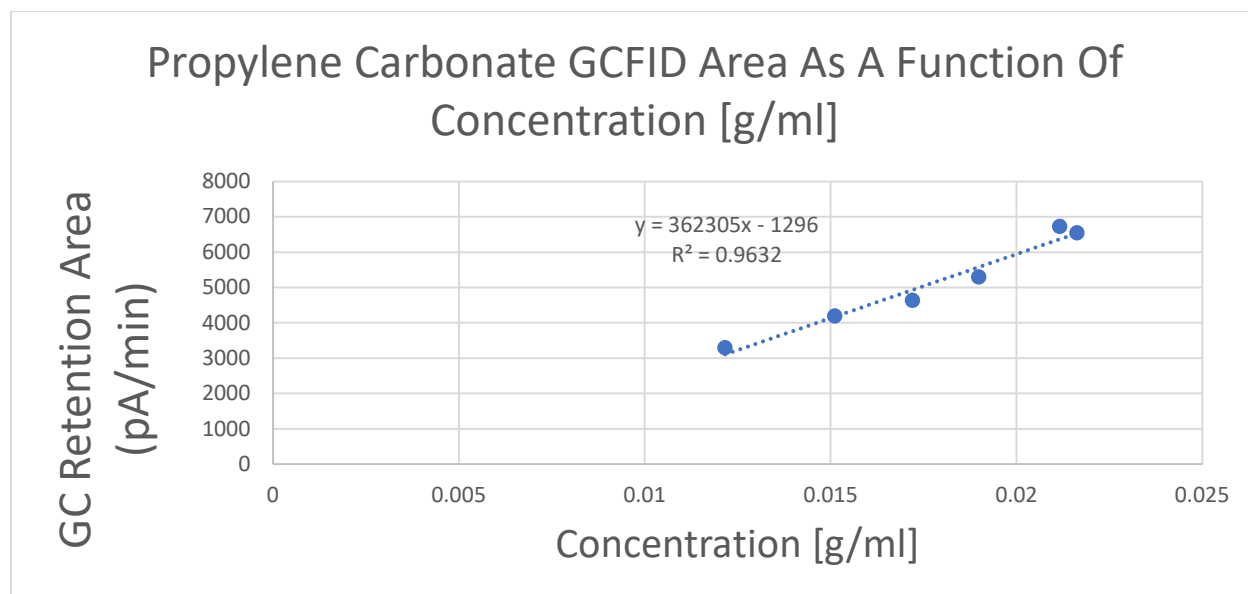


Figure 38. Standard curve for PC MilliporeSigma™ Supelco™ β-Dex 255 capillary GC column containing a chiral stationary phase of 2,3-diO-acetyl-6-O-TBDMS-β-cyclodextrin. Helium carrier gas, inlet temp. 250 °C, column temp. 205 °C, FID temp 300 °C, and continuous flow of 1ml/min.

Ethyl Acetate	
kp	0.105384531
at 95% confidence	
+/-	0.02863

mean	0.105384531
stdv	0.058439417
Conf.	0.05
size	16
Interval	0.028634788

Table 2. Statistical analysis of Kp value for ethyl acetate.

THF	
kp	1.26
	at 95% confidence
	+/- 0.49

mean 1.26  
 stdv 0.56  
 Conf. 0.05  
 size 5.00  
 Interval 0.49

*Table 3. Statistical analysis of Kp value for THF*

Propylene Carbonate	
kp	0.527569
	at 95% confidence
	+/- 0.13

mean 0.527568692  
 stdv 0.149905341  
 Conf. 0.05  
 size 5  
 Interval 0.13139541

*Table 4. Statistical analysis of Kp value for propylene carbonate.*

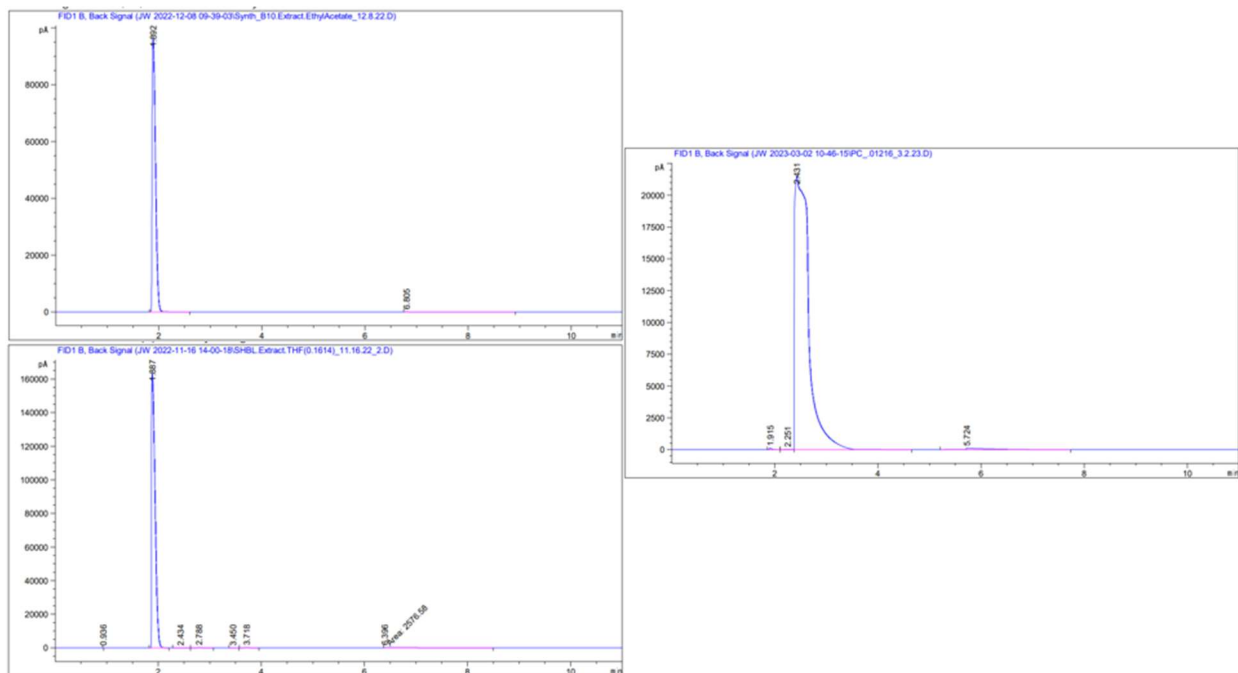


Figure 39. GC-FID peaks for EA (top), THF (bottom), PC (right). EA appears to be more selective in extraction of HBL from solution as there are only two peaks corresponding to the solvent and the HBL. With both THF and PC, additional peaks are identified which indicate extraction of unwanted byproducts which would require further processing for removal.

Process Area	Assumptions	Installed Cost	Reference
Production of HBL (ISBL)*		\$15,304,879	
<b>Totals</b>		<b>\$15,304,879</b>	
Warehouse	4.0% of ISBL	\$612,195	[43]
Site development	9.0% of ISBL	\$1,377,439	[43]
Additional Piping	4.5% of ISBL	\$688,719.56	[43]
<b>Total Direct Costs (TDC)</b>		<b>\$17,983,233</b>	[43]
Prorateable expenses	10.0% of TDC	\$1,798,323.31	[43]
Field expenses	10.0% of TDC	\$1,798,323.31	[43]
Home office & construction fee	20.0% of TDC	\$3,596,646.61	[43]
Project contingency	10.0% of TDC	\$1,798,323.31	[43]
Other costs (start-up, permits, etc.)	10.0% of TDC	\$1,798,323.31	[43]
<b>Total Indirect costs</b>		<b>\$10,789,940</b>	
<b>Fixed Capital Investment (FCI)</b>		<b>\$28,773,173</b>	
Land		\$1,800,000	[43]
Working Capital	5% of FCI	\$1,438,659	[43]
<b>Total Capital Investment (TCI)</b>		<b>\$32,659,832</b>	
*ISBL	Inside battery limit		

*Table 5. Total capital investment for the production of HBL.*

<b>Equipment</b>	<b>Installed equipment cost</b>	<b>Reference</b>
Pressure swing adsorption	\$113,844	[41]
Air Compressor	\$1,317,000	[41]
Seed trains	\$3,000,000	[43]
Hanging bag reactors	\$1,118,542	[42]
Centrifuge	\$569,000	[41]
Continuous stirred reactors	\$2,743,455	[41]
Extraction column	\$2,580,000	[41]
Distillation and Evaporation columns	\$3,863,000	[41]

*Table 6. Total process equipment costs for the production of HBL.*

		Source
Glucose	0.5 (\$/kg)	Personal communication
Ethyl acetate	1.5 (\$/kg)	ICIS Chemicals
Sodium citrate	2 (\$/kg)	PharmaCompass
Piperazine	32 (\$/kg)	PharmaCompass
HCl	0.179 (\$/kg)	ICIS Chemicals
NaOH	0.38 (\$/kg)	ICIS Chemicals
	5	
Natural gas price	(\$/MMBtu)	USEIA
	0.12	
Electricity cost	(\$/kWh)	USEIA
Operating Days	330	Assumption
Internal rate of return	10%	Assumption
Equity	100%	Assumption
Salvage value	0	Assumption
Plant life	20 years	Assumption

*Table 7. Operating costs and discounted cash flow analysis assumptions.*

## **ABOUT THE AUTHOR**

Justin O'Neil Parks Waters was raised in Connecticut by his father Ian Eric Waters, and his mother Elcheva Mychelle Parks Waters. He attended Robert E. Fitch Senior High school, graduating in 2005. From there, he attended the University of Connecticut where he earned a B.A. in foreign language.

After undergraduate studies, he joined the U.S. Army as a transportation and logistics officer, attending Officer Candidate School. Upon commissioning, he served for three years on active duty at Fort Eustis. There, he worked as platoon leader, before being promoted to operations officer, and ultimately quickly ascending to Battalion S1. At the end of his active-duty period, Justin moved to Washington D.C. where he served an additional four years in the Army Reserves.

While in D.C. he worked as a market research analyst for the Health Industry Distributors Association, leading the Business Intelligence department. There he served as industry data expert, publishing annual market reports in six healthcare market segments.

In his spare time, he loves to read about cutting edge science. This passion culminated in an inevitable decision to return to school to pursue his dream of earning a degree in chemical engineering. Upon returning to school, he earned two STEM associates degrees before enrolling at North Carolina State University in a graduate level bridge program for non-science students transitioning into engineering. After completing the bridge coursework he transferred to the University of Maine where he spent two years working towards his M.S. in chemical

engineering. He is a candidate for the Master of Science degree in Chemical Engineering from the University of Maine in May 2023.